Processive Recoding and Metazoan Evolution of Selenoprotein P: Up to 132 UGAs in Molluscs

Janinah Baclaocos[1,†], Didac Santesmasses[1,2,3,†], Marco Mariotti[1,2,3,†], Katarzyna Bierła[4], Michael B. Vetick[5], Sharon Lynch[6], Rob McAllen[6], John J. Mackrill[7], Gary Loughran[1], Roderic Guigó[2,8], Joanna Szpunar[4], Paul R. Copeland[5], Vadim N. Gladyshev[3] and John F. Atkins[1]

1 - Schools of Biochemistry & Microbiology, *University College Cork, Ireland*
2 - Centre for Genomic Regulation (CRG), *Barcelona Institute for Science and Technology, Barcelona, Catalonia, Spain*
3 - Division of Genetics, *Department of Medicine, Brigham and Women's Hospital and Harvard Medical School, Boston, MA 02115, USA*
4 - Laboratory of Bio-Inorganic Analytical Chemistry and Environment, *LCABIE- IPREM, Technopole Helioparc, 2 Av. President Angot, 64053 Pau, France*
5 - Department of Biochemistry and Molecular Biology, *Robert Wood Johnson Medical School, Rutgers University, New Brunswick, NJ 08854, USA*
6 - School of Biological, *Earth & Environmental Sciences, University College Cork, Ireland*
7 - School of Physiology, *University College Cork, Ireland*
8 - Universitat Pompeu Fabra (UPF), *Barcelona, Spain*

Correspondence to Marco Mariotti: *mmariotti@bwh.harvard.edu.*
https://doi.org/10.1016/j.jmb.2019.08.007
Edited by Dan Tawfik

Abstract

Selenoproteins typically contain a single selenocysteine, the 21st amino acid, encoded by a context-redefined UGA. However, human selenoprotein P (SelenoP) has a redox-functioning selenocysteine in its N-terminal domain and nine selenium transporter-functioning selenocysteines in its C-terminal domain. Here we show that diverse *SelenoP* genes are present across metazoa with highly variable numbers of Sec-UGAs, ranging from a single UGA in certain insects, to 9 in common spider, and up to 132 in bivalve molluscs. *SelenoP* genes were shaped by a dynamic evolutionary process linked to selenium usage. Gene evolution featured modular expansions of an ancestral multi-Sec domain, which led to particularly Sec-rich SelenoP proteins in many aquatic organisms. We focused on molluscs, and chose Pacific oyster *Magallana gigas* as experimental model. We show that oyster *SelenoP* mRNA with 46 UGAs is translated full-length *in vivo*. Ribosome profiling indicates that selenocysteine specification occurs with ~5% efficiency at UGA1 and approaches 100% efficiency at distal 3′ UGAs. We report genetic elements relevant to its expression, including a leader open reading frame and an RNA structure overlapping the initiation codon that modulates ribosome progression in a selenium-dependent manner. Unlike their mammalian counterparts, the two SECIS elements in oyster *SelenoP* (3′UTR recoding elements) do not show functional differentiation *in vitro*. Oysters can increase their tissue selenium level up to 50-fold upon supplementation, which also results in extensive changes in selenoprotein expression.

Introduction

Selenium is an essential trace element for humans and for many other organisms [1]. The major reason for its importance in living systems is its occurrence in catalytic sites of certain oxidoreductases: selenium-mediated reactions are thought to be readily reversible and hence the presence of selenium in proteins and certain tRNAs enables them to resist permanent oxidation [2]. Facilitation of resistance to

oxidative inactivation relates to its irreplaceable role in mammalian interneurons in preventing fatal epileptic seizures [3]. Selenium is also important in other aspects of human health such as male fertility [4,5]. The deleterious consequences of deviations from physiologically important environmental levels of selenium in mammals are well known, including extreme selenium deficiency (e.g., in some regions of China until dietary supplementation) and its toxic levels (e.g., in parts of the American West) [6,7]. However, less is known about the significance for human health of intermediate dietary levels such as those found in North American and European soils and derived food. Suboptimal selenium levels are thought to have been important in prior era mass extinction events [8].

The biological effects of selenium in mammals are largely mediated by its incorporation in specific proteins (selenoproteins) in the form of selenocysteine (Sec), the 21st encoded amino acid [9,10]. With a small number of interesting bacterial exceptions [11], Sec is encoded by UGA (due to frequent switching from RNA to DNA in this report, UGA will also be used for the DNA counterpart rather than TGA). While in standard decoding UGA specifies translation termination, its meaning is dynamically redefined to specify Sec in response to mRNA-specific recoding signals and multiple specialized accessory factors. In eukaryotes, the most important such mRNA signal is part of the 3′UTR folded into a structure termed SECIS (*s*elenocysteine *i*nsertion *s*equence) [12,13]. SECIS elements have a quartet of non-Watson–Crick base pairs [14,15] to which the protein SECISBP2 binds, and ribosomal protein L30 is also relevant to the interaction [16,17]. SECISBP2 binds the specialized elongation factor (EEFSEC) for selenocysteinyl-tRNA [18–23]. Additional trans-acting factors including eIF4a3 [24] and nucleolin [25] are important regulators of the Sec incorporation machinery. In some eukaryotic selenoprotein mRNAs, cis-acting structures known as Sec redefinition elements (SREs) are also found adjacent to the UGA [26–29].

Nearly all selenoproteins contain a single Sec, which is often at the active site. One clear exception is selenoprotein P (SelenoP) [30] that contains a single redox-active Sec in its N-terminal domain [31–33] and, in addition, multiple Secs in its C-terminal domain [34–36]. Full-length SelenoP serves a selenium transport function of critical importance for the brain, testes, and other tissues [4,37]. Apart from limited bioinformatic studies in amphioxus and sea urchins [38,39], SelenoP has been almost exclusively investigated to date in vertebrates. *SelenoP* mRNAs are unique among vertebrate selenoproteins in having two rather than one SECIS element in their 3′UTRs [40] (although some isoforms of human *SelenoP* mRNA have only one SECIS [37]). More recently, in addition to SRE-like elements, the *SelenoP* RNA structure termed initiation stem loop (ISL) was identified with proposed roles in translation initiation [41].

The majority of known selenoproteins have non-Sec-containing orthologs in other organisms wherein Sec is replaced by cysteine (Cys), suggesting that, for several functions, the advantage of selenolate-*versus* thiolate-based catalysis is not universal or that the use of Sec is also associated with deleterious consequences that can outweigh its catalytic advantage. The presence of orthologs with either Sec or Cys has been exploited for bioinformatics studies that have yielded extensive information on these proteins. For example, analyses of selenoproteomes have uncovered trends in Sec utilization across species [38] including massive independent selenoprotein losses in insects, higher plants, fungi, and protists [42–44]. Aquatic organisms have been shown to have generally large selenoproteomes, in contrast to terrestrial organisms, which have reduced them through losses of selenoprotein genes or Sec to Cys replacements [33]. For studies of genes encoding SelenoP, the issue is more complicated as it involves the use of multiple UGA codons. Such bioinformatic analysis of vertebrate *SelenoP* has revealed up to 22 in-frame UGA codons in some genes [45]. The largest number of UGAs identified bioinformatically so far in an invertebrate *SelenoP* mRNA is in the purple sea urchin *Strongylocentrotus purpuratus*, where 28 are present [33]. Here we carried out detailed analyses of *SelenoP* in metazoa revealing unexpected diversity of its forms and new regulatory aspects of multiple codon redefinition.

Results

SelenoP genes and Sec codon locations in metazoa

The computational search of metazoan genomes and transcriptomes resulted in 3464 predictions of *SelenoP* sequences, which after filtering yielded 1228 high-quality non-redundant genes (Methods). *SelenoP* was found in ~50% of metazoan genomes, clustering in specific lineages. *SelenoP* was missing from the genomes of tunicates, Platyhelminthes, all nematodes except *Trichinella*, and the great majority of arthropods (Fig. 1). Computational "translations" revealed the presence of sequences encoding Sec-rich C-terminal domains in SelenoP in various metazoan lineages. Diverse C-terminal domains were observed in vertebrates, echinoderms, arachnids, cnidarians, and various members of Lophotrochozoa (lineage including Annelida, Nemertea and molluscs, among others). To investigate the evolution of *SelenoP* and the emergence of C-

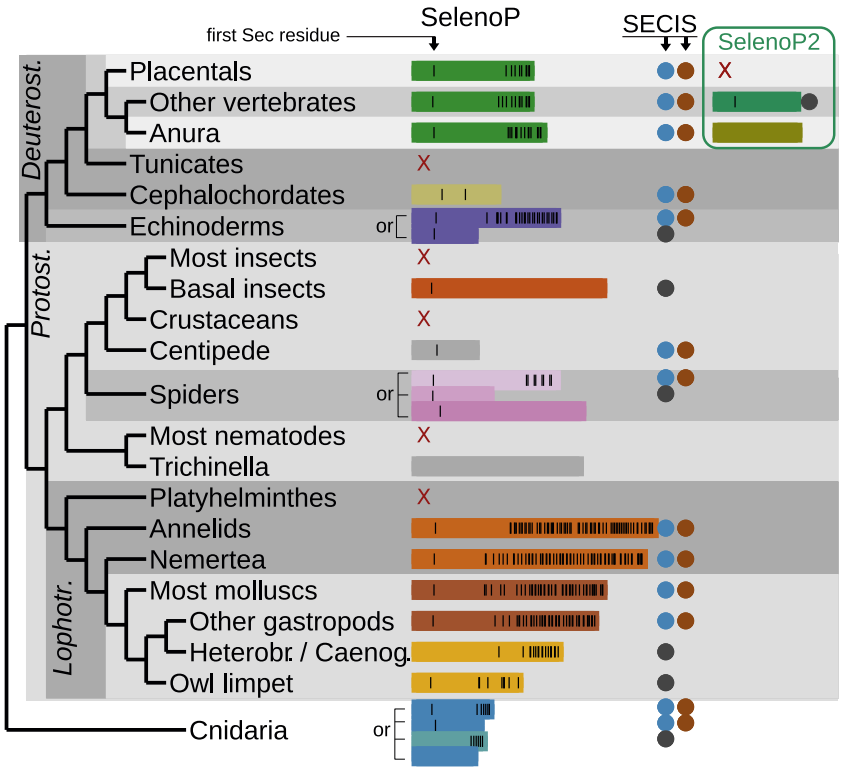

Fig. 1. *SelenoP* genes identified in metazoan species. The figure shows a summary of the *SelenoP* genes found in metazoa. Genes are represented as rectangles colored by phylogenetic cluster (see Fig. 2). Sec residues are indicated as vertical black lines, SECIS as circles. Note that this representation does not capture the remarkable diversity within each group, particularly in the number of Sec residues (Fig. 2). In the species tree on the left, some lineages are indicated with abbreviations: deuterostomes, protostomes, Lophotrochozoa. Abbreviations were used also for Heterobranchia and Caenogastropoda (molluscs, gastropods; Supplementary Note 3).

terminal domains, we reconstructed a gene tree derived from the sequence alignment of the N-terminal portion of SelenoP proteins (Supplementary Fig. 1). This tree was used to define 14 phylogenetic clusters of encoded proteins. Integrated with the species tree (Fig. 2), this was used as backbone to inspect the evolutionary conservation of various sequence fetures including the position of the first Sec-encoding UGA codon (UGA1), clustering of multiple UGAs in the distal segment, two SECIS and an exon intron boundary just 3′ of UGA1 (although this last information is available only for genomic predictions, with fewer gene sequences obtainable in invertebrates than in vertebrates). The alignment of representative sequences for each protein cluster is presented in Supplementary Fig. 2.

Vertebrates

Vertebrate genomes contain two main classes of *SelenoP* genes: (1) an ortholog of human *SelenoP* with two SECIS elements and a Sec-rich C-terminal domain, hereafter referred as *SelenoP1* for clarity, and (2) a shorter, single-Sec codon paralog hereafter termed *SelenoP2* (but also known as *Sepp2*, *SelPb*). As previously reported [45], *SelenoP2* is present in all vertebrates except placental mammals, where it was lost. *SelenoP1* and *SelenoP2* share the same intron structure and form sister clades in the gene tree. This suggests that the two genes originated by gene duplication approximately at the root of vertebrates; likely, the two genes were retained after a whole genome duplication [46]. The Sec codon of *SelenoP2*, which corresponds to the first Sec codon of *SelenoP1* (hereafter referred as UGA1), was converted to a Cys codon in two vertebrate lineages, Anura (group of Amphibia including frogs) and Galeomorphii sharks (cartilaginous fish) (Supplementary Note 1). The number of Sec codons in *SelenoP1* varies considerably across vertebrates. Hystricomorph rodents (i.e., guinea pigs, mole rats) had the lowest number (5–7 codons). At the other end, three species of *Seriola* amberjack fish (*S. dumerili, S. rivoliana, S. quinqueradiata*) had 33–37 (*S. lalandi* had instead only 25). However, the highest number of putative Sec-UGAs in a vertebrate, 49, was observed in *Oreobates cruralis*. In this species of robber frog, SelenoP1

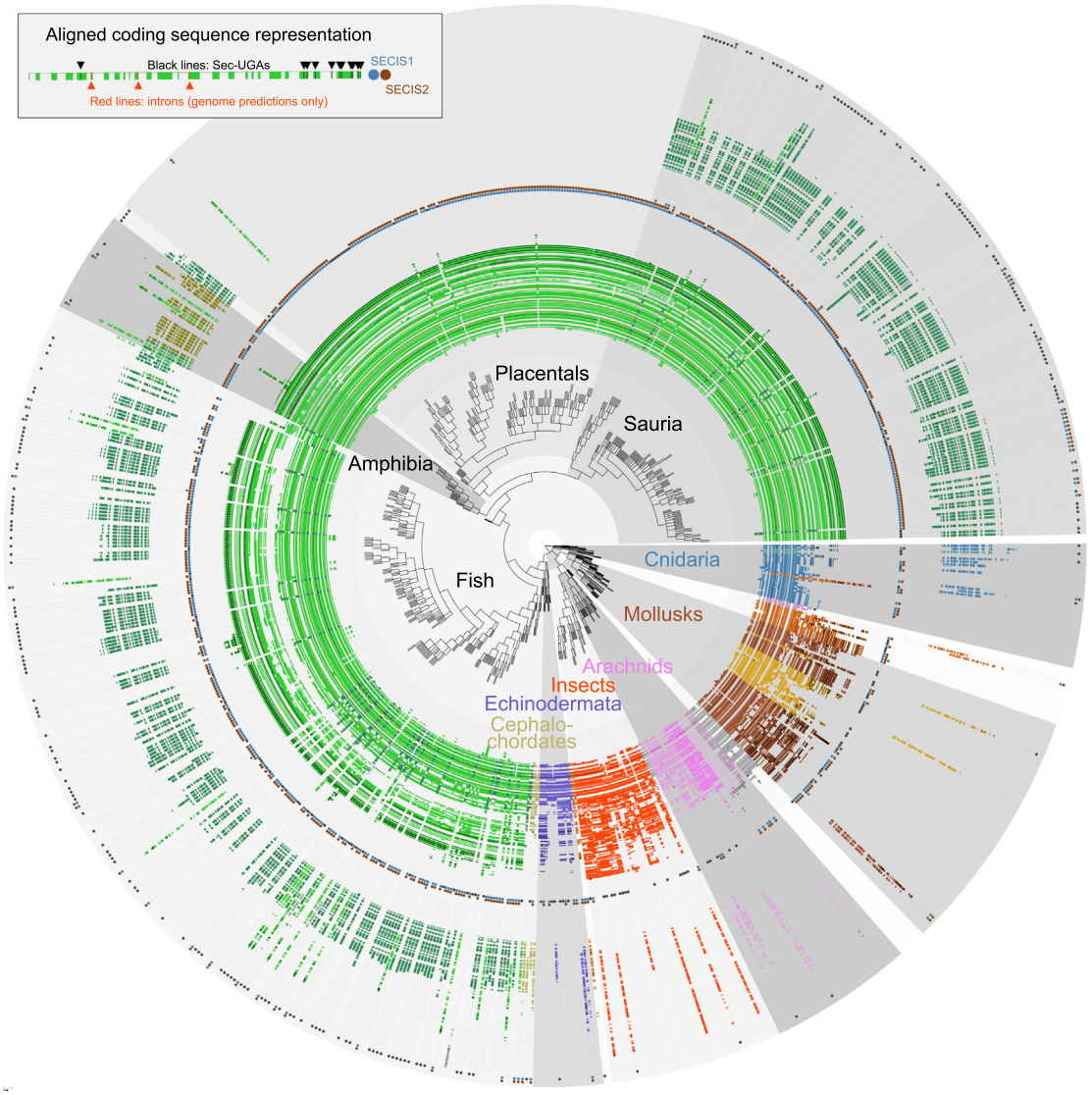

Fig. 2. Tree representation of *SelenoP* in diverse metazoan species. Color coding of individual genes displayed follows phylogenetic clustering (Methods). This representation (legend top left) displays the positions of putative Sec-UGAs as black lines, and introns as red lines (for predictions in genomes only). Next to each gene, predicted SECIS elements are shown in blue and brown circles. The inner circle shows the *SelenoP* gene with the highest number of UGAs per species; the outer circle shows the gene with the second highest amount, if present; in a few cases, more than two genes were identified, and they were omitted in this representation. Note that only genes passing all filters (Methods) are displayed here; genes apparently missing may have been filtered out for low quality sequence (e.g., many non-placental vertebrates appear to lack *SelenoP1* or *SelenoP2*).

contains a repeated C-terminal region, so that its mRNA includes ~28 more UGAs than its closest relatives. However, since we observed this extension in a single species and sequence source, we cannot exclude that this is an artifact of transcriptome assembly.

Cephalochordates

The selenoproteome of cephalochordate *Branchiostoma floridae* (amphioxus) has been previously reported [39]. Its *SelenoP* mRNA has multiple Sec codons and two SECIS elements. However, instead of the encoded protein having a Sec-rich C-terminal tail like other species, amphioxus SelenoP is formed by tandem repetitions of the thioredoxin-like domain. In the mRNA, each of the Sec codons is located in a homologous context to UGA1 of human *SelenoP*. Through our genomic searches, we found that this gene structure is conserved in the cephalochordate lineage.

Echinoderms

SelenoP was previously reported in the echinoderm *S. purpuratus* (purple sea urchin) [33] Indeed, our search identified *SelenoP* in all echinoderms, forming a single monophyletic cluster in the reconstructed tree. As in *S. purpuratus,* the *SelenoP* of these other species contains multiple Sec-UGAs and two SECIS elements with the highest number of UGAs, 43, being identified in the brittlestar *Amphiura filiformis*. However, several other species (e.g., sea cucumber, *Parastichopus parvimensis*) contain a *SelenoP* gene with a single UGA, which is at the characteristic UGA1 position, and a single SECIS.

Molluscs

We identified *SelenoP* in all main classes of molluscs: bivalves, cephalopods, and gastropods. With few exceptions ascribed to imperfect assembly quality, all molluscan *SelenoP* genes encode a long Sec-rich C-terminal domain, with clear homology within molluscs. The highest number of putative Sec codons in any *SelenoP* sequence searched to date is in the freshwater mussel *Elliptio complanata*. With 131 in-frame UGAs, Sec is predicted to be the second most abundant amino acid in the encoded protein. We confirmed Sec-UGA numbers by RT-PCR and Sanger sequencing (Supplementary Note 2). This revealed one additional Cys codon converted to a Sec codon raising the number to 132; variants with increasing numbers of UGAs may be segregating in the population. While *E. complanata* constitutes an outstanding outlier, high Sec counts were present in most bivalves (e.g., 46 in Pacific oyster, *Magallana gigas*), and in many cephalopods (e.g., 66 in the golden cuttlefish *Sepia esculenta*) and gastropods (e.g., 45 in the veined rapa whelk *Rapana venosa*; 14 in the edible periwinkle *Littorina littorea*). Within gastropods, we observed UGA1 converted to Cys in the lineage comprising Heterobranchia and Caenogastropoda, although its precise phylogeny is difficult to solve (Supplementary Note 3). Interestingly, we did not detect more than one SECIS for *SelenoP* in this lineage, despite featuring multiple distal Sec-UGAs.

Other Lophotrochozoa

Molluscs belong to the phylum Lophotrochozoa, which also includes Platyhelminthes (flatworms), Nemertea (ribbon worms), and Annelida (segmented worms). While we did not find *SelenoP* in Platyhelminthes, the other two categories of worms have highly Sec codon rich *SelenoP* genes. For example, 65 in-frame UGAs are present in *SelenoP* of the bootlace worm *Lineus longissimus* (Nemertea) and 66 in *Platynereis dumerilii* (Annelida). Two SECIS elements were identified in most multi-Sec codon *SelenoP* genes in worms. In the reconstructed gene tree, worm sequences formed a single cluster that also included brachiopods (e.g., *Lingula anatina*). This cluster includes a few genes with a single UGA and one or no SECIS (although this could be due to poor assembly quality). The predicted C-terminal Sec-rich domain has homology between Mollusca, Nemertea, and Annelida, supporting common inheritance of Sec codon-rich *SelenoP* within Lophotrochozoa.

Nematodes

SelenoP is missing in the great majority of nematodes, with the sole exception of the *Trichinella* genus (an early-branching lineage of parasites). Several *Trichinella* species have a distant *SelenoP* homolog that has a Cys codon in place of UGA1. While in some cases there are 2–3 in-frame UGAs at the end of the coding sequence (CDS), they are not conserved in this genus, and no SECIS candidate is detected in these genes (with a single possible exception). It is likely that SelenoP is not a selenoprotein in *Trichinella*, and that other nematodes either lost this gene entirely or diverged beyond our recognition power.

Insects

We did not find *SelenoP* in the great majority of insects, including fruit flies, mosquitos, and beetles. However, *SelenoP* was identified in various early branching insect lineages, including Zygentoma (silverfish, firebrats), Odonata (dragonflies, damselflies), Blattodea (cockroaches, termites), Phasmatodea (stick-insects), and Paraneoptera (lice). These genes typically feature a single SECIS and UGA1 (Sec) and form a single cluster in the reconstructed protein tree (Supplementary Fig. 1). Beyond the N-terminal thioredoxin-like domain, insect *SelenoP* genes encode a ~550-residue C-terminal domain with no similarity to any characterized protein. All the above-mentioned insect lineages contain the Sec machinery, which is not ubiquitous in this class: several branches of holometabolous insects (Endopterygota) lost it in independent events [42,47]. Consistently, we did not find *SelenoP* in holometabola, with the sole exception of some Hymenoptera (wasps). In these selenoproteinless species, UGA1 is not conserved and there is no detectable SECIS, indicating that this remote hymenopteran SelenoP homolog is not a selenoprotein.

Other arthropods

We observed a remarkable diversity in arthropods. Crustaceans appear not to contain *SelenoP*. However, the centipede *Strigamia maritima* has a

SelenoP with a single UGA, situated at the characteristic UGA1 location. *SelenoP* genes from arachnida (spiders, ticks, mites) formed three phylogenetic clusters, likely representing a single orthologous group with diverse divergence rates (Supplementary Note 4). Interestingly, we did not find any SECIS elements in SelenoP genes of Acariformes (arachnids). This group included both genes with an in-frame UGA corresponding to UGA1 and genes with diverse codons in its place. Future research will clarify whether these genes encode selenoproteins, or perhaps if their mRNAs are translated through a distinct mechanism of UGA recoding.

Cnidaria

We found *SelenoP* in many Cnidaria (early branching lineage of marine metazoans). Upon protein tree reconstruction, cnidarian sequences formed two distinct phylogenetic clusters. The smallest group consisted of sequences from Scyphozoa (true jellyfish such as *Aurelia aurita*, which has paralogs in both clusters). Genes in this cluster have classic position UGA1 replaced with a Cys codon, a distal region with multiple UGAs, and apparently only one SECIS element. The other and largest cluster encompassed hydrozoans, box jellyfish, sea anemones, and corals. The majority of genes in this cluster carry a single UGA at the characteristic UGA1 position, and either one or two SECIS elements. A few genes in this cluster had instead multiple UGAs, both at the UGA1 position and in the distal region (homologous to Scyphozoa), and two SECIS elements.

Protein homology and modularity in SelenoP

Our analyses highlighted a number of differences between *SelenoP* genes of vertebrates and invertebrates. We thus proceeded to a comprehensive computational characterization aimed to elucidate their evolution. All SelenoP proteins identified have a similar N-terminal thioredoxin-like domain. However, Sec-rich tails have no obvious homology across distant metazoan groups: Blastp does not detect significant homology (*e*-value < 0.01) between the human SelenoP tail and that of any other phylogenetic cluster representatives. Aiming to clarify the evolution of *SelenoP*, we developed an improved procedure to detect local homology in protein sequences (Methods, Supplementary Fig. 3). Our method can detect both inter- and intra-sequence similarities, which is relevant because various multi-Sec tails features obvious modularity, with similar motifs repeated in tandem (Supplementary Fig. 2). Our results are shown in Fig. 3. All SelenoP proteins match each other for the first ~200 residues, corresponding to the thioredoxin-like domain. At the C-terminal domain, several proteins contained shifted matches with themselves, indicating modularity. Besides the aforementioned thioredoxin-like repetition in cephalochordata, the simplest case was in spider (arachnida). Here, Sec residues located in the C-terminal region, formed by four repetitions of a 2-Sec motif, are separated from the thioredoxin-like domain by a region that also featured self-similarity. The sequences of molluscs, echinoderms and marine worms presented outstanding modularity, with high counts of matches both with themselves and with each other. Importantly, we detected local homology between some of these repetitions and the C-terminal domain of human SelenoP1 (Fig. 3; expanded in Supplementary Fig. 3C). These matches span the entire length of the human multi-Sec tail, from the Sec encoded by UGA2 to the end of the protein. Even with our conservative *e*-value cut-off, it is possible that some of these alignments are spurious and do not represent true homology, since SelenoP distal sequences have a very skewed C/U-rich composition. However, our finding of a perfectly conserved TESCQU motif between human and bootlace worm *L. longissimus* (Supplementary Fig. 3C) is a strong indication that genuine homology is present. Notably, the alignments between the human and invertebrate sequences contained the binding site of ApoER2 in vertebrates, with its key motif ZQZ (Z representing Sec or Cys). Human SelenoP has two nearby ZQZ sites, the second of which was shown to be essential for ApoER2 binding [32]. Pacific oyster and bootlace worm have 14 and 29 ZQZ motifs, respectively, most of which have a similar sequence context to the second site in human. Among the rest of selected SelenoP representatives, only purple sea urchin *S. purpuratus* has ZQZ; a single occurrence is located at the very end of its sequence, but its context does not resemble its human counterpart. The significance of these results for the evolution of *SelenoP* is presented in Discussion.

Invertebrate SelenoP translation in supplemented rabbit reticulocyte lysates

In order to monitor Sec-incorporation with T7-transcribed *SelenoP* mRNA, we used co-translational ^{75}Se labeling in rabbit reticulocyte lysate (RRL) supplemented with rat C-terminal domain of SECISBP2 (CT-SECISBP2) [22,27,48,49]. This system was previously shown to support translation of vertebrate full-length SelenoP [50], but has never been tested with invertebrate SelenoP. We selected a few SelenoP representative sequences for tests of *in vitro* translatability. The house spider (*Parasteatoda tepidariorum*; arthropod, arachnid; 9 Sec-UGAs and two SECIS) mRNA yielded a product of ~70 kDa, whose synthesis was dependent on the presence of CT-SECISBP2 (Fig. 4A, green asterisk).

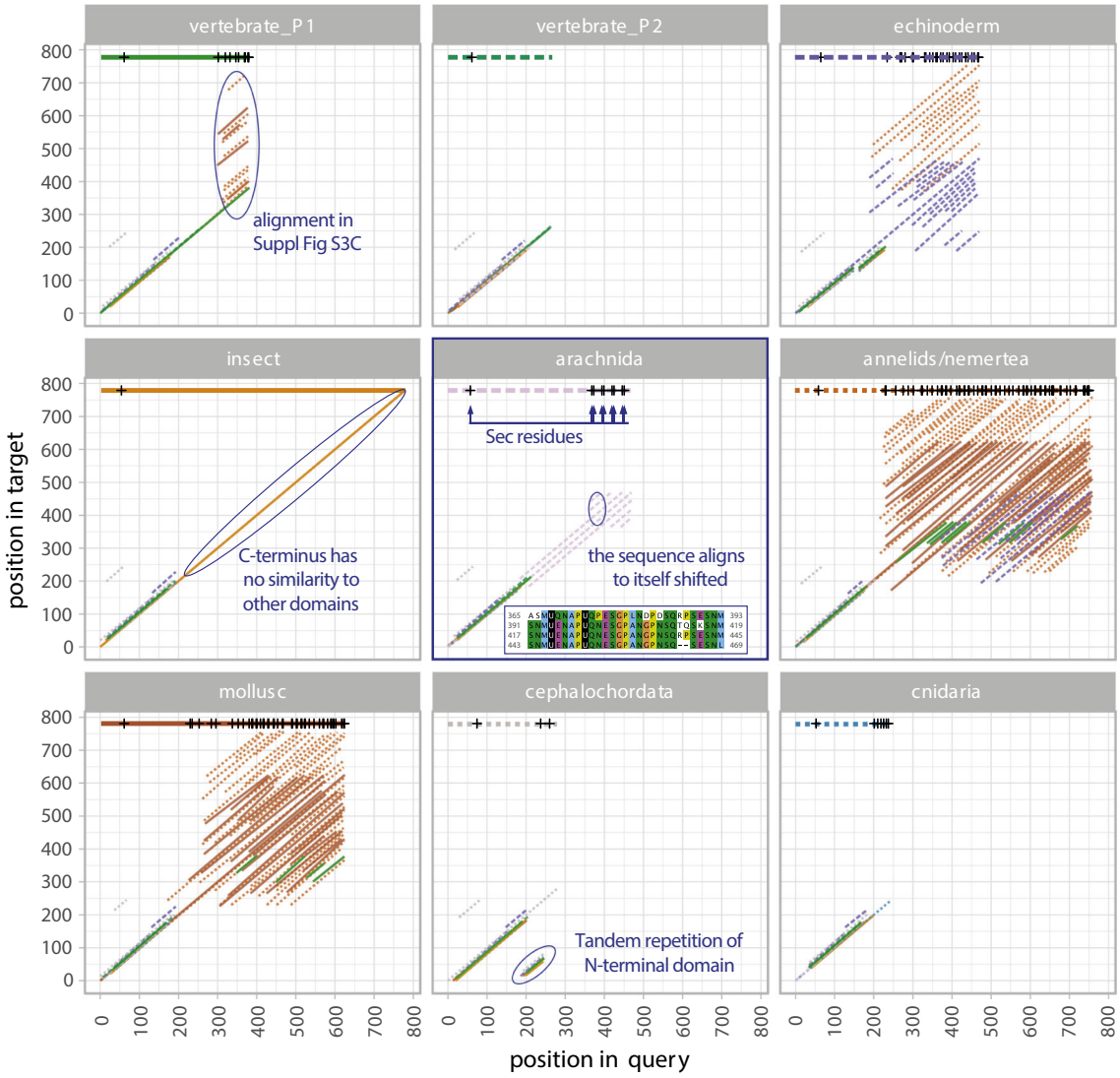

Fig. 3. Homology and modularity in SelenoP protein sequences. The plot represents local homology matches identified between SelenoP representatives (Methods). The central panel is used to illustrate the plot meaning. Each panel consists of a dot-matrix-like plot, with each diagonal line representing a match between a query (e.g., arachnida; *P. tepidariorum*) and a target (either the query itself or any other representative), color coded by target sequence. At the top of each panel, a horizontal line shows the query length and the positions of Sec residues. In arachnida, the C-terminal domain with 8-Sec consists of 4 repetitions of a 2-Sec module, resulting in multiple matches of this sequence with itself. Some C-terminal domains show high modularity (intra-sequence matches), and also homology with other representatives (inter-sequence matches). We identified matches of vertebrate SelenoP tail (human; top-left panel) with regions of invertebrate Sec-rich C-termini; these are shown in Supplementary Fig. 3C.

Interestingly, its migration on gels was slower than its predicted full-length molecular weight (ca. 50 kDa). This may be due to its proline-rich amino acid composition (Supplementary Fig. 2) or may indicate the presence of post-translational modifications. The owl limpet (*Lottia gigantea*; mollusk, aquatic gastropod; Sec-UGAs and one bona fide SECIS) mRNA yielded no detectable radiolabeled product (not shown). However, Pacific oyster (*M. gigas,* formerly known as *Crassostrea gigas* [52]; mollusk, bivalve; 46 Sec-UGAs, two SECIS) mRNA yielded a labeled product of ~30 kDa, conditional on the addition of CT-SECISBP2 (Fig. 4B, red asterisk). The estimated molecular weight of this product approximates that expected from decoding the mRNA up to the fourth UGA codon. In addition, a CT-SECISBP2-dependent diffuse band was also observed (Fig. 4B, red bracket). Since UGA positions in the distal region of oyster SelenoP are in very close proximity, the

diffuse band could indicate premature termination within the UGA-rich distal segment.

Effect of oyster SelenoP sequence elements on in vitro translation

A search in the CDS of *SelenoP* from six bivalves, each containing more than 45 UGAs, revealed the potential for formation of a stem loop structure close to the initiation codon. Because of the degree of conservation, presence of sequence covariation, and analogy to a known vertebrate counterpart [41], we term this element ISL. In *M. gigas* the ISL spans CDS positions 40 to 160 from the annotated AUG (Supplementary Fig. 4). The possibility that the ISL acts as a barrier and perhaps influences initiation efficiency at the AUG prompted further *in vitro* translation experiments with *M. gigas SelenoP* mRNA. In order to assess the effect of the ISL and other sequence features, we generated and tested several oyster *SelenoP* variants. *In vitro* transcribed mRNAs corresponding to each of these variants were translated in RRL labeled with ^{75}Se and supplemented with CT-SECISBP2. First, we noticed that the *M. gigas SelenoP* open reading frame (ORF) began with the start codon in a weak Kozak context (c.GAUGcG), which differs from the oyster transcriptome consensus (AaaAUGgc, closely similar to that identified in mammals). We thus replaced this with a strong Kozak context AcCAUGGca. There was no product difference, except perhaps a slight increase in the amount of the termination product (Fig. 4B, lane 4; Supplementary Fig. 5A, lane 4). Second, we identified a small 5′ Leader ORF (16 codons, beginning 73 nt 5′ of *SelenoP* start codon), whose AUG is in a modest Kozak context (c.GAUGAA), which is expected to cause 30% to 40% of the scanning subunits to initiate translation [53–55]. Upon removal of the entire native 5′ leader (yet retaining 110 nt of vector sequence as 5′UTR), there was a modest reduction in the amount of the termination product (Supplementary Fig. 5A, lane 5). Third, the disruption of sequence complementarity in the ISL through synonymous codon mutations resulted in the absence of detectable ^{75}Se product (Supplementary Fig. 5A, lane 6; note that the product due to ribosomes terminating at UGA1 would not have been detected by ^{75}Se labeling). An additional experiment using ^{35S}Met labeling (Supplementary Fig. 5B, lane 7) detected the presence of significantly reduced early termination product at UGA1 upon ISL mutation, suggesting that initiation efficiency is reduced but not entirely abolished. Fourth, sequence inspection revealed that *M. gigas SelenoP* mRNA has an RNA structure homologous to vertebrate SRE2/3. It is located in CDS positions 1585–1705, spanning UGAs 31–35 in *M. gigas* (Supplementary Fig. 4). Deleting the sequence from UGA11 to UGA46 yielded no SelenoP-specific radiolabeled product (Supplementary Fig. 5A, lane 7). While this deletion removes the SRE2/3, the occurrence of initiation (Supplementary Fig. 5B, lane 9) means that the lack of ^{75}Se-labeled product likely reflects long range mRNA folding being relevant to Sec specification.

Lastly, we focused on SECIS elements. *M. gigas SelenoP* mRNA contains two SECIS in its 3′UTR with signature conserved motifs also found in vertebrates (Supplementary Fig. 4). As in vertebrates, the two oyster *SelenoP* SECIS elements also differ by an additional structural element, found in SECIS 1 (type II) but not SECIS 2 (type I). Oyster SECIS elements function to permit full-length ^{75}Se-labeled product from zebrafish *SelenoP* CDS (Supplementary Fig. 5A, lane 8). Appending oyster SECIS 1 or oyster SECIS 2 to the zebrafish CDS yielded full-length product with similar efficiency (Supplementary Fig. 5A, lanes 9 and 10), suggesting that each oyster individual SECIS element has high affinity to rat SECISBP2, to a similar degree as the zebrafish combined SECIS elements (Supplementary Fig. 6). The absence of functional distinction between oyster SECIS 1 and 2 in this heterologous system contrasts with their vertebrate counterparts. The "Berry model" for vertebrate SelenoP translation asserts that SECIS 2 functions to reprogram UGA1 for Sec insertion, while SECIS 1 acts for processive Sec insertion at the distal UGAs. This model was not proposed in absolute terms, and much evidence from vertebrate *in vitro* protein synthesis, cell culture and mice with specific mutants of the endogenous gene, supports the proposed preferential action of the two SECIS elements [37,51,56,57].

Attempting to improve *in vitro* translation of oyster SelenoP, we considered using its native Sec recoding machinery. We identified a single homolog of human *SECISBP2* in the *M. gigas* genome, consistent with earlier findings in various invertebrates. We refer to this gene as *SECISBP2*, although it is also homologous to *SECISBP2L* (Supplementary Note 5) [58,59]. We purified a recombinant full-length *M. gigas* SECISBP2 (Supplementary Fig. 7C). In RRL supplemented with oyster SECISBP2, instead of rat SECISBP2, oyster *SelenoP* mRNA did not yield detectable ^{75}Se-labeled product (not shown). In the same system, translation of rat *SelenoP* mRNA did result in UGA specification of Sec but likely only by UGA1 (Supplementary Fig. 7D). Our results suggest partial incompatibility between the translation machinery of oysters and vertebrates, and/or unknown oyster trans-acting components lacking in RRL, necessary for processive Sec incorporation. While meaningful for mechanistic insights, our *in vitro* experiments fell short of definitive evidence of full-length oyster SelenoP synthesis. In quest of it, we turned to a different experimental model.

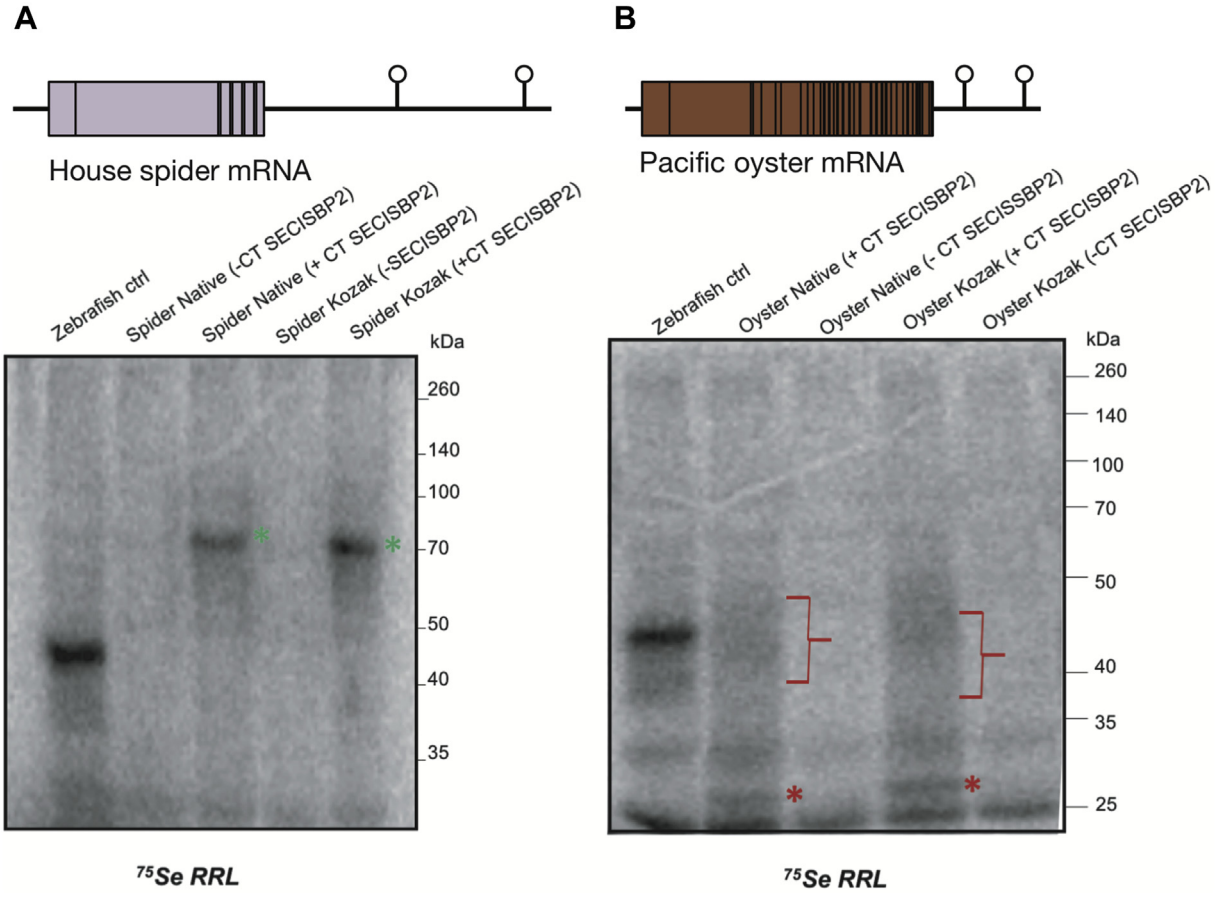

Fig. 4. Invertebrate *SelenoP* mRNA translation in CT-SECISBP2 supplemented RRL. On top, the structures of *SelenoP* mRNA of (A) house spider, *P. tepidariorum* and (B) Pacific oyster, *M. gigas*, are displayed, including the location of Sec-UGAs within the CDS and SECIS elements in the 3′UTR. Below, the results of their *in vitro* translation experiments are shown. We tested mRNAs with either their native initiation context or an added Kozak consensus, with or without supplemented CT-SECISBP2. The first lane shows the translation product of zebrafish *SelenoP* mRNA as control for processive Sec incorporation [51]. A low molecular weight product (~25 kDa) was observed across all experiments even in the absence of added mRNA (Supplementary Fig. 5) and was ascribed to RRL background. Green asterisks (A) denote a radiolabeled product corresponding to a full-length spider SelenoP. Red asterisks (B) denote oyster SelenoP termination product at UGA 3 or 4, and red bracket highlights a diffuse product(s) indicative of possible termination between UGAs 4–46.

Selenium biology of the oyster *M. gigas*

As our analyses revealed highly Sec-rich *SelenoP* genes in molluscs, and bivalves in particular, we performed *in vivo* experiments aimed to characterize the role of selenium in mollusk biology. Pacific oyster *M. gigas* was chosen for its widespread importance in the human food industry, and the availability of genome and transcriptome sequences [60,61]. We identified 32 selenoprotein genes in the genome sequence of *M. gigas,* along with a complete set of factors required for selenoprotein synthesis (*tRNA-Sec*, *PSTK*, *SEPSECS*, *SECISBP2*, *EEFSec*, and *SEPHS2*) (Supplementary Table 1). All of these genes were also identified in a comprehensive transcriptome assembly [61], providing evidence for their expression. In addition, a transcript encoding a SelenoW protein (SELENOW.1) was identified in the transcriptome. The sequence was supported by both RNA-seq and riboseq, but was missing in the genome assembly. Oyster selenoproteins belonged to 22 distinct families. These encompassed all selenoprotein families previously described in invertebrate metazoans [39], including three families not found in vertebrates: AHPC, MSRA, and DSBA. In addition, we identified a Sec-containing radical *S*-adenosyl methionine (*RSAM*) gene (Radical SAM/Cys-rich domain; Interpro IPR026351) in *M. gigas*, including a SECIS downstream of CDS. RSAM selenoproteins had never been observed in metazoa but had been previously reported in bacteria [62] and in a single-cell eukaryote, the harmful bloom alga

Aureococcus anophagefferens (UniProt F0XY08) [63]. Sequence searches revealed numerous RSAM selenoproteins in bivalves and other metazoan lineages (Supplementary Fig. 8). Crustaceans, bivalves. and most cnidarian species contain Sec in their RSAM protein, while echinoderms possess a Cys homolog. We identified two genes belonging to the *SelenoP* family in *M. gigas*. The second gene, here referred to as oyster *SelenoPb*, also contains two SECIS elements, but it is shorter and has fewer UGAs than its paralog *SelenoP* (Supplementary Note 6). Our analysis suggests that oyster *SelenoPb* appeared by tandem duplication in the *Crassostrea* lineage, which includes *M. gigas*.

Selenium uptake and accumulation in oyster tissues

Oysters feed on natural phytoplankton by filter-feeding. They are known for their capacity to filter microscopic food sources from water as well as their ability to bioaccumulate sediments, nutrients and even pollutants from their environment [64]. To investigate the effects of selenium concentration on the *M. gigas* selenoproteome, and particularly the translation of SelenoP, we carried out an oyster selenium supplementation where the microalgae food source (*Tetraselmis* sp.) was grown in Se-rich medium by the addition of 28.9 μM (5 mg/L) final concentration of sodium selenite. This concentration was previously suggested to allow optimal Se uptake without inducing toxicity to algal cells [65,66]. Guided by preliminary analyses, we chose to focus on adult male oysters (Supplementary Note 7). Two groups of 10 individuals were distributed to separate tanks and fed weekly for 6 weeks with equal amounts of microalgae pre-grown with or without Se supplementation, and were then analyzed by inductively coupled mass spectrometry (ICP-MS; Methods). Total selenium levels in tissues of selenium-supplemented oysters increased 20-fold on average compared to non-supplemented controls (Table 1), whose levels were also compared to those in farmed marine mussels, *Mytilus edulis* (Supplementary Table 2). Remarkably, individual oysters accumulated 50-fold higher selenium levels than in the control group without mortality. Other material from the supplemented tank, including oyster non cytoplasmic debris, sea water, and the algae that served as food source, also showed elevated selenium levels (Supplementary Table 3).

Effects of selenium supplementation on selenoproteome expression

To assess the effects of selenium concentration on selenoprotein gene expression, we performed RNA sequencing (RNA-seq) and ribosome profiling (riboseq) of oysters with and without selenium supplementation. While RNA-seq characterizes overall transcript levels, riboseq can elucidate ribosome occupancy and potential regulation at specific regions, by mapping ribosome-protected fragments (RPFs) to mRNAs. For each group, we selected whole body tissue from two oysters that had similar levels of total measured selenium (average 3.4 and 17 μg/g for non-supplemented and supplemented, respectively). The soft tissues of each pair were pooled and prepared for sequencing. A preliminary assessment of our ribosome profiling data was performed through metagene analysis (Supplementary Note 8). Despite a noticeable difference between supplementation groups, our data featured considerable triplet periodicity and quality suitable for downstream analysis. We thus quantified expression of Sec machinery and selenoprotein genes and compared them with the whole oyster transcriptome (Supplementary Fig. 9). Transcripts with low coverage were discarded (Methods).

Our results show a general trend of an increase in selenoprotein mRNA abundance (Fig. 5, red) and RPFs (Fig. 5, blue) upon selenium supplementation, consistent with previous reports of ribosome profiling on selenium-supplemented mice [67,68]. Translation efficiency, estimated as RPF abundance relative to mRNA abundance, was actually reduced in oyster selenoproteins upon supplementation (Supplementary Fig. 9C), because the transcript level increase (up to a 7-fold in individual selenoproteins) was greater than the RPF increase (about 3-fold). The observations in oyster differ from reports in mice wherein Se has a greater effect at protein level than at transcript level [67]. As for Sec machinery genes, we found no selenium-dependent regulation on *EEFSEC*, while *SEPHS2* was upregulated and *SEPSECS*, surprisingly, downregulated (Fig. 5).

Analogously to previous research [67,69], we obtained a surrogate estimate of Sec UGA-redefinition efficiency (URE) calculated as the ratio of RPF density downstream to upstream of UGA (Methods). URE represents the proportion of ribosomes that translated past the Sec-UGA codon compared to those that initiated translation. It cannot be calculated for selenoproteins with UGA-Sec near to the very 5′ or 3′ end of CDS. Consistent with previous reports of Sec-UGA redefinition in mice, we observed that the majority of selenoproteins exhibited a low URE, although there were several exceptions (Supplementary Table 4). The analysis of ribosome profiling for oyster *SelenoP* is presented hereafter.

In vivo* translation of 46 Sec-UGA *SelenoP

Ribosome coverage of oyster SelenoP mRNA

Ribosome profiling allowed us to monitor oyster SelenoP translation *in vivo*. RNA-seq showed full

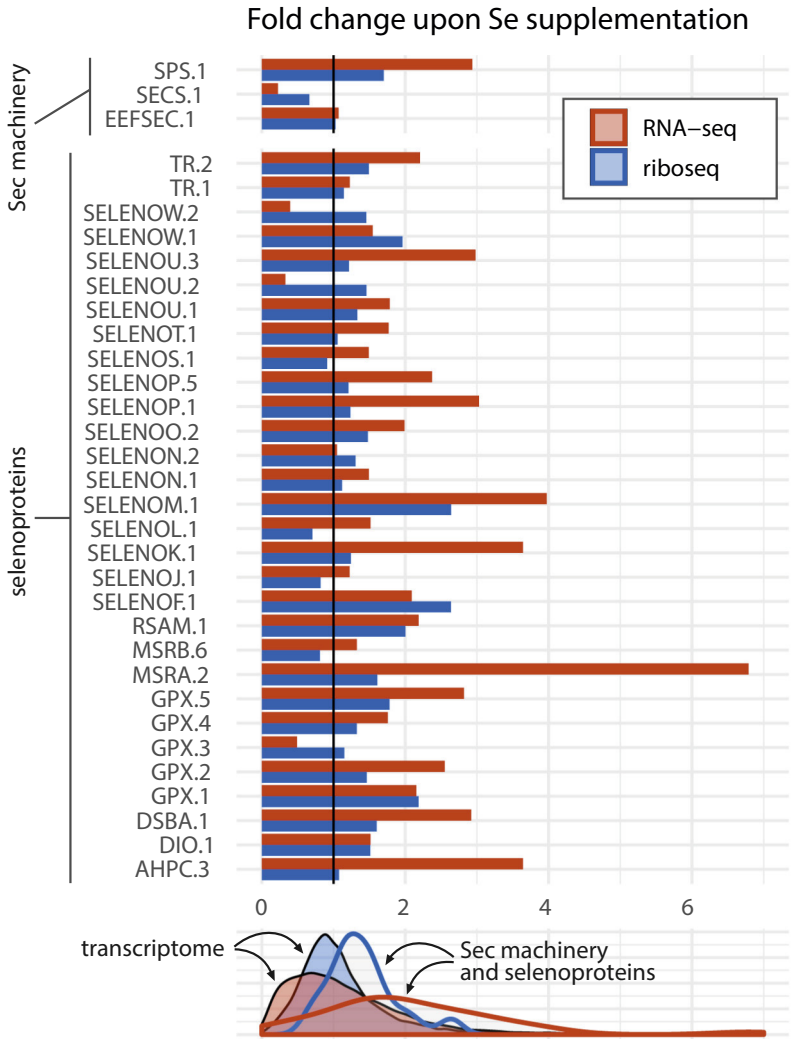

Fig. 5. Selenium supplementation effects on expression of oyster selenoprotein and Sec-decoding "machinery" genes. The gene expression response to selenium supplementation is expressed as the fold change in mRNA abundance from RNA-seq (red, RPKM) or ribosome footprints from riboseq (blue, RPFKM) between Se-supplemented and non-supplemented samples. Absolute expression values are shown in Supplementary Fig. 9. The bottom panel shows how selenoprotein and Sec machinery genes compare to the distribution of the whole oyster transcriptome. Supplementary Table 1 indicates the correspondence between oyster gene identifiers used here and human genes. Selenoproteins *DIO.2*, *SELENOH.1* and Sec machinery *PSTK.2*, *SBP2.117* were omitted from this analysis for low coverage.

coverage along its mRNA, including its 5′ 110-nt Leader, CDS, and 3′UTR, while riboseq was mostly limited to the CDS as expected (Fig. 6A). Notably, some RPFs mapped to a specific 61-nt region spanning the previously identified 5′ Leader ORF, supporting that it is translated. Ribosome coverage was only moderately greater in the sample derived from selenium supplemented tissue. In the non-supplemented sample, the most abundant fragments were mapped from 15 nt 5′ of the CDS start and sharply dropped 20 nt 3′ of it (Fig. 6A, green arrow). The ISL RNA structure was found 20 nt 3′ of the coverage drop (ISL at positions 37−157 from main ORF AUG). The amount of these fragments was greatly reduced upon selenium supplementation. Comparing the RPF coverage map for the two conditions, the fragments from the non-supplemented material were somewhat less abundant approaching UGA1 and some of their boundaries moderately shifted. Inferences from such complex patterns in profiling data merit caution, but the data showed a broad RPF accumulation prior to UGA1 that was also present in mammalian *SelenoP* ribosome profiling data [41,69]. We computed URE for UGA1 by comparing RPF density in the CDS 5′ of UGA1 to the density in the region between UGA1 and UGA2. The URE for the non-supplemented group was 5.6%, whereas that for the supplemented

Table 1. Selenium accumulation in oyster tissues

Individual oyster tissue	Non-supplemented			Supplemented		
	Av. Se per individual (μg/g)	SD	RSD	Av. Se per individual (μg/g)	SD	RSD
A	3.47	0.27	7.5	80.2	0.8	1.1
B	3.3	0.2	6.15	48.4	0.34	0.69
C	3.12	0.25	7.95	179	0.28	0.16
D	4.72	0.23	4.94	36.8	0.43	0.17
E	2.9	0.18	6.1	19.9	0.32	1.59
F				52.1	0.52	0.98
G				13	0.2	1.56
Average Se concentration per group (μg/g of tissue)	3.502			61.3		
Certified reference materials, National Research Council of Canada (NRCC)	***Av. Se μg/g***	***SD***	***RSD***			
NRCC Reference Material Site						
DORM-1[a]	1.46	0.03	2.27			
TORT-2[b]	5.64	0.09	1.68			

Total Se levels in whole body soft tissue from seven males fed a Se-enriched diet (A–G) and five from an unsupplemented control group (A–E), individually determined by ICP-MS, are shown together with their standard deviation (SD) and relative standard deviation (RSD). Values for certified reference materials are also indicated.

[a] Certified value: 1.62 ± 0.12 μg/g (dogfish muscle).

[b] Certified value: 5.63 ± 0.6 μg/g (lobster hepatopancreas).

group was 4.7% (Supplementary Table 4). Thus, selenium level does not exert a strong influence on UGA1 redefinition in oyster, unlike its mammalian counterpart [67,69]. The role of the pause site is considered in Discussion.

As introduced earlier (Supplementary Note 6), a second gene, termed oyster *SelenoPb* (SELENOP.1), was identified in *M. gigas* exhibiting high homology to *SelenoP*, 5′ of UGA1. However, we detected minimal RPF coverage 3′ of UGA1 in *SelenoPb* where the sequences are less homologous, suggesting that its expression levels were significantly lower, if not almost undetectable, compared to *SelenoP*. We therefore deduce that reads obtained in the presented *SelenoP* coverage map should accurately represent translation of its mRNA. The oyster RPFs map to the full length of the predicted CDS up to the UAG termination codon (Fig. 6A). This result strongly supports full-length 46 Sec-UGA *SelenoP* translation in *M. gigas*. Translation of UGAs 2–46 appeared to be continuous and processive as indicated by the absence of ribosomal pausing and approximately equal RPF coverage across the UGA-rich segment, comparable to that found for its mammalian counterpart translation, both *in vitro* [57] and in mice [67].

Detection of full-length oyster SelenoP by immunoblot

Portions of the lysates used for ribosome profiling were further employed for immunoblot analysis. Custom *M. gigas* SelenoP antibodies were raised against the N-terminal region encoded upstream of UGA1 (anti-NT SelenoP) and the C-terminal region encoded after UGA43 (anti-CT SelenoP). The antibodies were tested for peptide affinity and specificity (Supplementary Fig. 10). Both antibodies detected an immunoreactive product that migrated on SDS-PAGE at an apparent molecular weight of 68 kDa, matching the predicted molecular weight of full-length oyster SelenoP (Fig. 6B, red arrow). Full-length product appeared to increase upon Se supplementation, consistent with the observed increase in RPF abundance (Fig. 6B, C). Anti-CT SelenoP also recognized a very prominent product with an apparent molecular weight below 37 kDa. Since this was not recognized by the N-terminal specific antibody, it likely represents a non-specific protein (see below), although we cannot exclude possible proteolytic cleavage products.

^{75}Selenium labeling of oyster larvae

Human *SelenoP* contains 10 in-frame UGA codons, which can also specify Cys instead of Sec to some degree dependent on the selenium supply level [70]. Our attempts to immunoprecipitate endogenous SelenoP from oyster tissues using the custom antibodies were unsuccessful. Consequently, to monitor *in vivo* Sec incorporation in oyster SelenoP, proteins were extracted from ^{75}Se-labeled free-swimming 7- and 14-day larvae and analyzed by autoradiography (Fig. 7A) (preliminary experiments guided the choice of larval age; see Methods). A parallel Western blot with

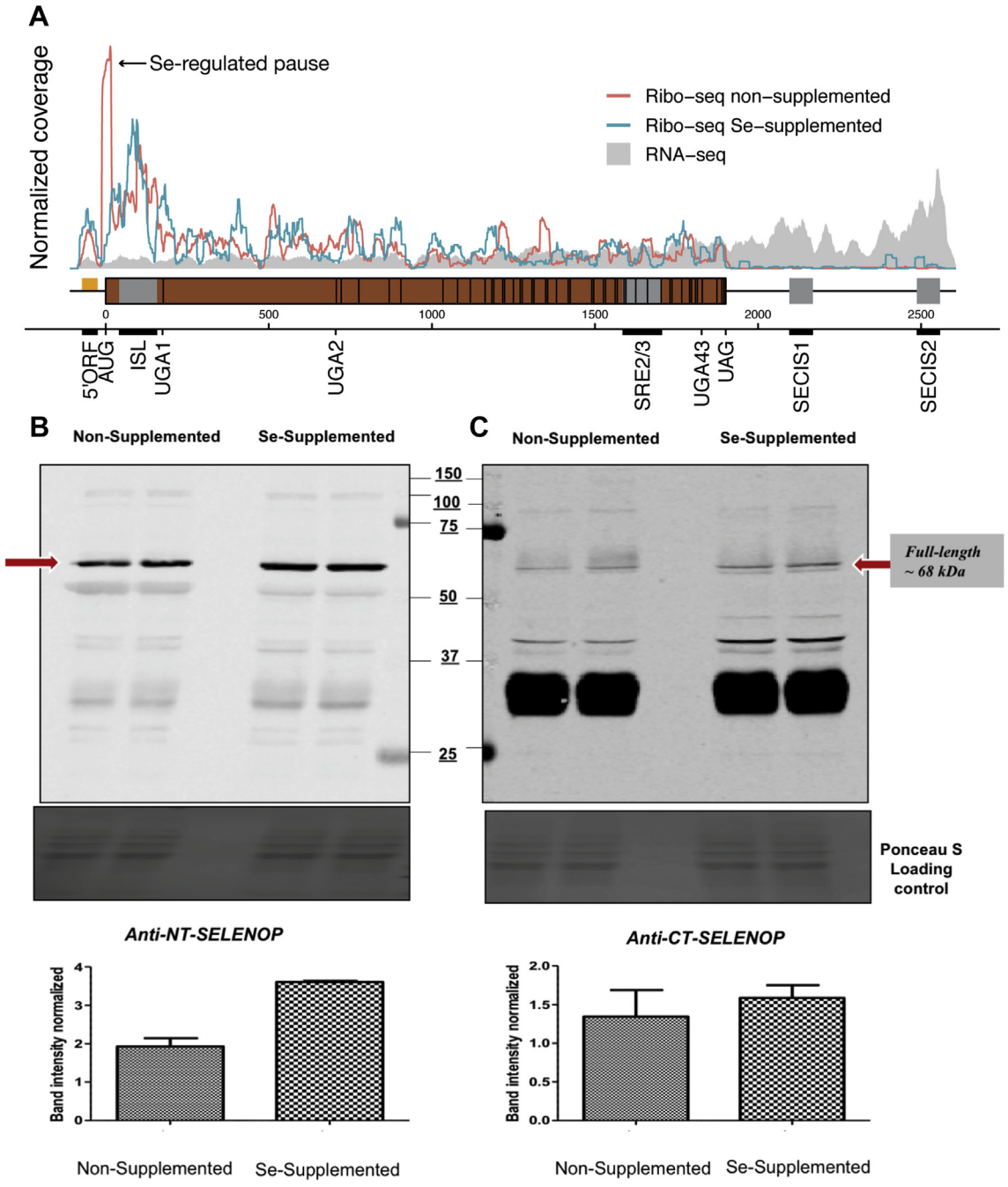

Fig. 6. Monitoring Pacific oyster SelenoP translation by ribosome profiling. (A) RNA-seq reads (gray) and riboseq RPFs (red for non-supplemented sample, blue for selenium supplemented) aligned to *SelenoP* mRNA positions. The coverage corresponds to full reads with no P-site offset, normalized to the total number of reads mapping to the mRNA. The RNA-seq reads were merged for the supplemented and non-supplemented. The 5′ leader ORF spans −55 to −22 nt positions (orange) whereas the main ORF is depicted as starting at position 0 (brown). Conserved RNA structures are shown in the gene model in gray. A selenium-regulated pause at initiation is indicated in the plot. (B, C) Immunoblot of the oyster tissue lysates used for library preparation using SelenoP custom antibodies targeting N-terminal (B) and C-terminal (C) portions of the protein. Red arrow indicates putative full-length protein detected at around 68 kDa. A densitometry graph (whiskers indicate SD of two technical replicates per sample) depicts the change in full-length band intensity in the non-supplemented vs Se-supplemented sample from each antibody; band intensity was normalized against a Ponceau-S loading control.

custom SelenoP antibodies detected a product at ~68 kDa, similar to that of the most intensely ^{75}Se-labeled protein. It corresponds to the predicted full-length *M. gigas* SelenoP. This is strong evidence for multiple Sec incorporation *in vivo*, and that SelenoP is the most selenium-rich protein in the *M. gigas* proteome. These results do not preclude the possibility of some level of specification of Cys at UGA sites, but if it occurs at all, it is very likely at a low level (also since some decoding of UGA as Cys in human cells is only detectable at low selenium [70]). The presence of lower molecular weight products detected by both autoradiography and anti-NT SelenoP (Fig. 7, blue arrows) suggests the presence of SelenoP termination products of 27 and 42 kDa derived from termination at UGA 2 and UGA 10–12, respectively. The additional radiolabeled products, not detected by our antibodies, should correspond to the other abundant selenoproteins. A counterpart of the <37-kDa product described in the last section was not detected.

Discussion

Evolution of Sec in *SelenoP*

Our characterization of *SelenoP* genes across metazoa brings a conundrum. We observed numerous short *SelenoP2*-like genes, encoding the thioredoxin-like domain, and long *SelenoP1*-like genes, encoding the thioredoxin-like domain and an additional C-terminal domain containing multiple Sec residues. There are two main evolutionary scenarios to explain these observations. The first involves common ancestry, wherein the occurrence of the multi-Sec sequence predates the split of these groups (i.e., *SelenoP1*-like is the ancestral state). In this scenario, the tail diverged extensively across groups, unlike the N-terminal thioredoxin-like domain, and also, the sequence encoding the tail was lost in *SelenoP2*-like genes. The alternative scenario involves convergent elongation: the various metazoan groups inherited a short *SelenoP* gene,

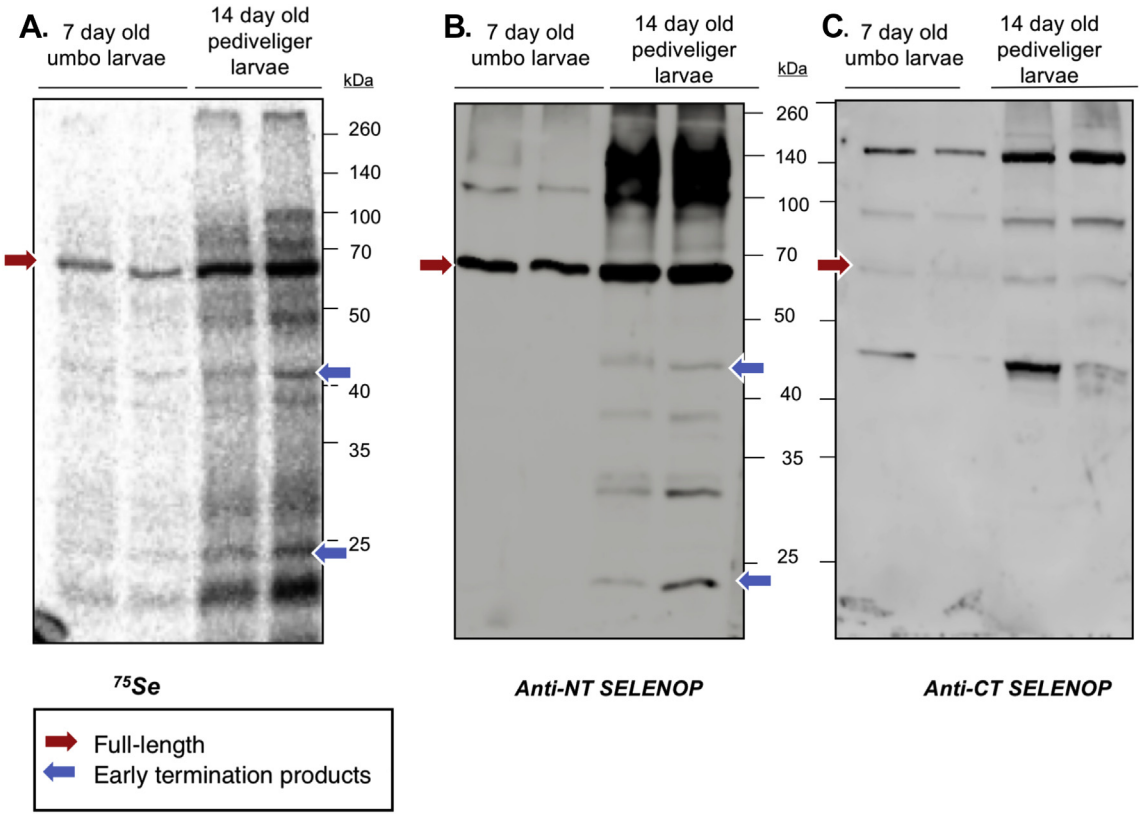

Fig. 7. ^{75}Se-labeled proteins in *M. gigas* larvae. (A) Autoradiography of radiolabeled proteins in 7-day and 14-day old oyster larvae. Each protein preparation was loaded in two lanes as technical replicates. (B) Anti-N-terminal and (C) anti-C-terminal SelenoP immunoblots of oyster larvae proteins. Red arrows indicate a radiolabeled and immunoreactive bands at an apparent molecular weight of 68 kDa, which is approximately the predicted size of full-length SelenoP. Blue arrows point to possible early SelenoP termination products detected by both autoradiography and parallel anti-NT SelenoP probing.

which underwent independent elongations to acquire non-homologous multi-UGA distal sequences (i.e., *SelenoP2*-like is the ancestral state). Based on the apparent lack of homology between the SelenoP tails of distant metazoans, we previously hypothesized that vertebrate *SelenoP1* originated by duplication of *SelenoP2*, implying that convergent elongation had occurred in other lineages [37,41]. However, our improved procedure for finding local homology allowed us to detect significant matches between the Sec-rich tail of human SelenoP and that of various invertebrates (Fig. 3). These findings support common ancestry as most likely scenario. To challenge this hypothesis, we reconstructed a phylogenetic tree of SECIS elements (Methods). If common ancestry is the correct explanation, human SECIS 1 should cluster with SECIS 1 of other species, with all SECIS 2 forming their own phylogenetic cluster. If instead convergent elongation occurred, the SECIS 1 and SECIS 2 sequences corresponding to each independent elongation should cluster together. Our reconstructed tree (Supplementary Fig. 11) features low bootstrap values (i.e., topology reliability), reflecting the challenge of phylogenetic reconstruction of RNA structures. However, we observed that SECIS 1 from vertebrates, marine worms, molluscs and some cnidaria cluster together, while their SECIS 2 form a distinct cluster, therefore further supporting the common ancestry scenario.

The multi-Sec tail of SelenoP shows obvious modularity in several lineages. The repeated motifs in any modular SelenoP are more similar to other occurrences within the same protein than to the sequence encoded by SelenoP in other metazoan groups. This suggests that these repetitions propagated in relatively recent times, after the evolutionary split between the various metazoan groups. Our observations indicate that, even in the context of common ancestry, independent events of elongation occurred to extend the C-terminal tail by repetition of a Sec-containing module. In other lineages, the tail was instead shortened or lost entirely. Altogether, our analyses point to a very dynamic process acting on the C-terminal tail, characterized by a fast rate of divergence, extension and contraction.

We believe that this process was driven by the environmental availability of selenium across biological niches, as well as the mutable reliance on selenium utilization by the various metazoan lineages. As a fundamental actor in selenium homeostasis of metazoa, SelenoP is tightly linked with selenium supply. At the level of individuals, SelenoP in plasma is a biomarker of selenium concentration that has been adopted as the reference standard in several European countries [71,72]. At the species level, the number of Sec residues in SelenoP significantly correlates with selenoproteome size, and thus with the degree of selenium utilization as previously reported [33] and confirmed by our analysis (Supplementary Fig. 12). It was previously hypothesized that selenium utilization is particularly important for aquatic life [38]. While the large selenoproteome of vertebrates apparently constitutes an exception, it was recently discovered that terrestrial vertebrates have relaxed evolutionary constraints on selenoprotein genes compared to fish [73]. Sec residues in the tail of SelenoP appear to follow a nearly neutral process of conversion to Cys. This may suggest that the large selenoproteome of mammals could be a legacy from our past in aquatic environments, slowly decreasing during our relatively slow evolution. Our own analyses of metazoan *SelenoP* are very much consistent with the aquatic hypothesis. While there are some exceptions (e.g., crustaceans lacking *SelenoP*), the proteins richest in Sec residues were all found in aquatic species. In particular, *SelenoP* evolution led to a truly remarkable number of Sec residues in this protein in molluscs and marine worms, with freshwater mussel *E. complanata* topping the list with 131/132.

Selenium biology in bivalves

Fish and shellfish are known for their high content of selenium, with the mussel *M. edulis* (blue mussel) scoring the highest selenium concentration in a recent survey across various marine organisms [74]. However, the role of selenium in the biology of these animals is virtually unexplored. Here, we characterized the oyster selenoproteome in detail and provided insights into selenium effects on gene expression regulation *in vivo*. We identified 32 selenoproteins in oyster, more than in mammals (25 selenoproteins) [45]. We provide the first report of an animal Sec-containing RSAM protein in oysters and found that it is also present in other bivalves, cnidarian, and crustacean species (while echinoderms possess a Cys homolog).

Supplementation studies revealed that the oysters can accumulate extremely high levels of Se in their tissues (Table 1), with an increase of up to 50-fold per individual. We further analyzed the effect of selenium supplementation on selenoprotein mRNA expression, translation and URE, using RNA-seq and riboseq. For these analyses, we used samples with around 6-fold increase in total Se levels. While more replicates and conditions would be necessary for precise quantitative assessments, our results show clear qualitative trends. In response to selenium, we observed a general upregulation of RPF counts, reflective of protein product abundance, with individual selenoproteins exhibiting up to a 3-fold increase. For *SelenoP*, RPF abundance correlated with protein abundance observed by immunodetection. At the transcript level, the trend of increased expression of selenoproteins was also

evident and featured an even stronger response (Fig. 5, Supplementary Fig. 9). This contrasts with earlier experiments in mice, where selenium supplementation caused a greater effect on translation, and mRNA levels were relatively unchanged upon selenium increase [67]. This discrepancy could be attributed to different rates of mRNA turnover, stability or susceptibility to nonsense-mediated decay (NMD) between organisms. Selenoproteins that presented the highest selenium response in mRNA levels in the Howard et al. study are known to be regulated during transcription, for example, *Gpx1*, which is a target for NMD [75,76], and *SelenoW*, which exhibits a high rate of mRNA turnover [77]. The difference observed in oysters might indicate the presence of an alternative regulatory system, perhaps a dedicated transcription factor sensing selenium levels. Further indications of translation playing a lesser role in selenium-response in oysters than in mammals come from the analysis of recoding efficiency. Oyster response to selenium was quite diverse across selenoproteins: not all selenoproteins exhibited enhanced URE or any strong 3′RPF increase, contrary to findings in mice [67].

Our analysis highlighted interesting differences in the regulation of the oyster selenoproteome by dietary Se compared to mammals. These are not surprising, given their long phylogenetic distance and many differences in physiology. It has been previously reported that, in oysters, accumulated minerals are compartmentalized resulting in a higher mineral turnover rate. Furthermore, subcellular compartmentalization of metals in bivalves may contribute to detoxification and may explain how they can circumvent toxicity as a result of bioaccumulation [64]. Oysters also possess an open circulatory system compared to a closed system in mammals. Such biological difference raises the question of whether the selenoproteins identified in oysters exhibit the same function. For instance, SelenoP in mammals has been strongly implicated in Se transport, as a hierarchy of selenium supplementation to tissues is achieved by preferential delivery of long SelenoP isoforms to brain and testis [32]. In oysters, we cannot exclude a possible role of SelenoP as a Se-storage protein due to the high Sec content in its C-terminal domain. Selenium and SelenoP have also been implicated in mercury chelation [78]. The high Sec content of SelenoP could be a possible adaptation to filter-feeding lifestyle, enabling oyster to tolerate high accumulation of toxic metals [79].

Upon supplementation, the remarkable increase in total selenium in tissues was accompanied by a more modest upregulation of selenoprotein levels. Thus, the levels of selenium in tissues cannot be accounted by just protein production, contrary to the situation in mammals where most increase in Se tissue level is directed to incorporation into selenoproteins [80,81]. This suggests the presence of additional molecular mechanisms for selenium accumulation, which may involve specialized protein machinery or non-protein components that bind Se, for example, low-molecular-weight selenocompounds or selenosugars.

Altogether, our work paves the way for investigating selenium biology in oysters and other molluscs. Considering the importance of these species in the food industry and their high selenium content, we expect that our research will prompt further studies to elucidate the function of selenoproteins and other aspects of selenium metabolism in these species.

Insights into the genetic decoding mechanism of oyster *SelenoP*

We identified a stem loop in oyster *SelenoP* mRNA, termed ISL, that is 37−157 nt 3′ of the main ORF start and 15 nt 5′ of UGA1. Its mammalian counterpart was shown to modulate translation initiation *in vitro*; analogous stem loops were characterized in non-selenoprotein mRNAs in bacteria [82]. In oyster, the function of ISL is selenium responsive. The oyster ribosome profiling shows an accumulation of abundant RPFs on the 5′ side of the ISL, indicative of blockage of ribosome progression. The peak of RPFs is observed only in non-supplemented samples, suggesting a regulatory mechanism sensing selenium level. Whether the ISL functions directly as a potential selenium riboswitch is outside the scope of the present work. Does it merely act as a "gate" for ribosome progression to avoid wasteful downstream translation? Alternatively, is it part of a mechanism for programming ribosomes at initiation so that they later decode UGA as Sec? In one model, a ribosome stalled at ISL would lead to its following ribosome having increased initiation potential at the main ORF start codon. Leader ORF translation may be relevant, but extensive work outside the scope of the present study is needed to assess significance. Disruption of the block when selenium (or perhaps toxins) became plentiful could lead to a burst of downstream translation and potentially SelenoP synthesis. However, the ribosome profiling of living oysters shows only a 1.5-fold increase of main ORF translation under conditions of a 6-fold total selenium increase, and Western blot analysis on tissues with more elevated selenium also does not show a dramatic increase (Supplementary Fig. 13). Also, there is not a substantial increase of leader ORF RPFs on selenium supplementation. While future studies involving selenium depletion are desirable, a paradoxical result was obtained with the heterologous *in vitro* translation experiments: 5′UTR deletion and synonymous codon substitution to disrupt the pairing involved in the ISL led to reduced

levels of initiation *in vitro* (Supplementary Fig. 5B, lanes 5 and 6, respectively).

Our heterologous *in vitro* translation experiments revealed some degree of interchangeability in the Sec incorporation factors and *SelenoP* mRNA elements between invertebrates, fish, and mammals. For instance, full-length translation of spider SelenoP with nine Sec residues was achieved in RRLs with reconstituted rat CT-SECISBP2 indicating that all the factors necessary for its translation are present in this system. In contrast, while oyster *SelenoP* mRNA also yielded Se-labeled product, it was not full length and only a product corresponding to termination at ~UGAs 3 or 4. Replacement of the SECIS elements in zebrafish *SelenoP* mRNA with either both or single, oyster counterparts and translation in reconstituted RRL showed that either oyster SECIS was equally able to support full-length translation (Supplementary Fig. 5A, lanes 8, 9, and 10). With caution in extrapolating from this heterologous system, this may mean that invertebrate *SelenoP* SECIS 1 and 2 are more functionally interchangeable than their mammalian counterparts. Another example of likely divergence involves *SECISBP2*. Invertebrates have a single gene in this family and vertebrates have two, *SECISBP2* and *SECISBP2L*. The former is a primary binder of SECIS elements and mouse conditional deletions gene revealed a significant reduction in mRNA-levels with retention of Sec specification [69,83]. The function of *SECISBP2L* is still unclear. Further research will be necessary to untangle the functions of the two paralogs and also the differences with the oyster ortholog seen in our heterologous experiments.

Ribosome programming for UGA redefinition to Sec is a complex process where much is left to be understood. What features may be relevant for SelenoP, where translation is further complicated by progressive recoding of multiple UGAs? In standard decoding, UGA as well as other stop codons (UAG and UAA) are decoded by protein release factors and this is a slow process compared to the decoding of sense codons by cognate aminoacyl-tRNA. The relatively lower rate of competing release factor-mediated termination may be significant for UGA1 specification of Sec. However, while the critical feature(s) for the SECIS protein complex programming of ribosomes remains unclear, multiple features may be facilitatory. SRE1, an mRNA structure close to UGA1 is not required but is relevant to Sec specification efficiency [41]. The deleterious effect found in the work reported here, of deleting from UGA 11−16, is consistent with the possibility that particular long-range mRNA folding is relevant to bringing a SECIS complex in proximity to a ribosome close to UGA1. Prior results also pointed to a relevant long-range mRNA structure [41,84,85]. The ISL is also a candidate for playing a role in ribosome programming, but this requires further exploration. Another possible facilitator involves interactions between the exon junction protein complex (EJC) and SECIS elements. A likely constituent of the complex, eIF4a3 is a selective negative regulator of selenoprotein synthesis and binds type I, but not type II SECIS elements in mammals [24,86]. Notably, there is a conserved exon/intron junction 26 nts 3′ of *SelenoP* UGA1 (of potential NMD relevance, this distance is smaller than 50 nt from UGA1; all the remaining UGAs are in the last exon). In one model, binding of eIF4a3 in the EJC to *SelenoP* SECIS 2 (type I), which is involved in redefinition of UGA1, may serve to facilitate localization of SECIS 2 for later replacement association with the oncoming ribosome. Such a potential mechanism cannot be obligatory since UGA1 can be recoded from mRNA generated from constructs lacking the intron, yet the high level of termination observed with those constructs [56] suggests that it may be relevant for improved efficiency. We analyzed the conservation of the exon/intron junctions in metazoan *SelenoP* genes, focusing on our set of predictions from genome sequences (Supplementary Fig. 14). Our analyses highlighted seven cases in which the first intron was lost. Three such cases were represented by UGA1-containing SECIS-lacking *SelenoP* genes identified in Acariformes, possibly translated by a Sec-independent mechanism (Supplementary Note 4). Notably, three other cases of intron loss were concomitant with substitution of UGA1 by a standard codon. It is tempting to interpret this observation as supportive of a facilitatory role for the EJC, as UGA1 substitution and loss of SECIS may have led to a lack of selective pressure to retain an EJC complex close to 3′ to at the former site of UGA1. In mice with deletions of endogenous SECIS 2, SECIS 1 can mediate some UGA 1 redefinition [37,41] and in part because of this there remains the possibility that the exon intron junction location is relevant in a subsidiary manner to the redefinition of UGA1 in WT conditions.

UGA is inferred to be an efficient terminator for standard decoding since it is the terminator for approximately 22% of *M. gigas* genes. Oyster ribosome profiling revealed inefficient (<5%) redefinition of *SelenoP* UGA1 but approximating to 100% efficiency for 3′ UGAs. In addition to the ribosome profiling results, the corresponding full-length translation of oyster SelenoP was demonstrated by metabolic Sec incorporation into oyster SelenoP with ^{75}Se labeling of oyster larvae, along with a parallel Western blot with anti-NT and anti-CT SelenoP antibodies. Given the larger numbers of distal UGAs in many cases and the proximity of these UGAs to each other (there are several occurrences of just one codon separating two UGA codons), we consider models involving the SECIS

complex tracking with, or acting as a once off ribosome "switch" [87], to be more appealing than separate contacts with a SECIS complex at each UGA. While there is good evidence from zebrafish to mammals for the general validity of the Berry model (UGA1 redefinition mainly enabled by SECIS 2, and redefinition of 3′ UGAs by SECIS 1), we have no experimental data relevant to whether this model is applicable for invertebrates. However, our experiments showed that both SECIS elements of oyster *SelenoP* supported progressive Sec incorporation *in vitro* of a zebrafish construct, suggesting that such SECIS specialization is not present in oyster. While there has been substantial debate about whether there are subsets of ribosomes free of mRNA that are specialized for translating particular mRNAs, decoding multiple UGAs in *SelenoP* as Sec is the most striking example of mRNA-linked ribosome specialization. Elucidation of the mechanisms involved in this mRNA-linked specialization, including by structural studies, will be a difficult but rewarding challenge.

Methods

SelenoP gene finding, phylogeny, and filtering

Gene prediction was carried out with the program Selenoprofiles v3.5c [88], which employs a protein alignment profile to scan nucleotide databases and find genes belonging to the same family. Due to its peculiar encoded C-terminal Sec-rich domain, *SelenoP* is particularly difficult to predict. This domain contains various stretches of repetitive sequences, resulting in lots of spurious hits in non-homologous repetitive regions of genomes during the very first step of Selenoprofiles (Blast search). We thus forced Selenoprofiles to perform the initial Blast search using only the conserved N-terminal domain. A second challenge derives from the C-terminal domain of SelenoP having no apparent similarity across various lineages, which hinders their discovery by homology. The 3′ portion of *SelenoP* genes can be found by looking downstream of regions with similarity to the N-terminal domain; in genomes, however, this is hampered by the potential presence of intervening introns. To remedy this, we searched abundant transcriptomic data (listed below) and used results to build a profile alignment containing representative SelenoP sequences across diverse lineages. This permitted the finding in genomes of homologous sequences encoding C-terminal domains. The newly created profile is now included in the Selenoprofiles package. In all our searches, we completed gene structures by extending homologous matches upstream (to the farthest AUG before any stop codon) and downstream (allowing UGA codons, but not any other stop). In total, we searched 1159 NCBI genomes, 1375 NCBI Transcriptome Shotgun Assemblies (TSA; all those available from metazoa excluding mammals and holometabolous insects), and 70 transcriptomes [89] from diverse lineages of lophotrochozoa. Our searches resulted in 3464 *SelenoP* gene predictions in total across all sources. Upon their inspection, we noticed that this set was highly redundant, with nearly identical multiple entries for the same genes, and included poor quality sequences, with incomplete gene structures and predictions from putative contaminations. We thus proceeded to filter and process these predictions through a number of analyses, described below, in order to obtain a bona-fide *SelenoP* set.

We aligned peptide sequences with ClustalO v.1.2.1 [90] then we processed them to merge those coming from the same genes, with the following procedure. First, for each species, we detected clusters of predictions referring to the same transcript, defined as presenting at least 96% identity (excluding terminal gaps) in their CDS. Only one representative was kept for each cluster. Often, such predictions complemented each other, in that they shared a common region, but each individually lacked the N-terminal or C-terminal encoding sections; in these cases, a new consensus sequence was produced to span the full gene sequence. Next, we processed the resulting alignment to keep only one isoform per gene. We detected clusters of predictions from the same species sharing a stretch of at least 120 nearly identical (96%) nucleotides in their CDS; we selected the longest prediction for each group, and we dismissed the rest. Throughout this procedure, we reduced our *SelenoP* set down to 1917 predictions. Next, we split the alignment in N- and C-terminal encoding sections, the former ending with sequence encoding the KDDFLIYDRCG motif in human, roughly corresponding to the end of SelenoP conservation across metazoan lineages. We thus built a protein tree using the N-terminal section, employing the routine "standard_trimmed_raxml" in ETE3 [91,92], and we employed it as backbone for a number of analyses, including a "phylogenetic filtering" procedure (explained below). Proteins from vertebrates formed a clear monophyletic cluster in the tree; thus, we split this portion of the tree from the rest for visualization purposes.

We proceeded to filter our raw prediction set using the resulting phylogenetic tree topology. The first phylogenetic filtering step was motivated by the observation of a number of *SelenoP* predictions clustering with species very distant from their annotated source organism. For example, the transcriptomes of *Crassostrea hongkongensis* and *angulata* (bivalves) contained SelenoP sequences nearly identical to *Sus scrofa*. These genes cluster together with all mammalian SelenoPs in the protein

tree and are very distant from other sequences from bivalves. Both transcriptomes were deposited by the same researchers. We concluded that these genes are not actually present in *Crassostrea*, and that they derived from sequence contamination from pig. The inspection of the protein tree highlighted numerous analogous cases. We thus defined a score for each gene, expressing the consistency between the protein tree and the taxonomy of source organisms. We considered 10 "phylogenetic neighbors" for each protein, defined as those with shortest distance in the reconstructed tree, and their annotated NCBI taxonomy (e.g., for *C. hongkongensis*, this would consist of the following 15 units: "*cellular organisms*; *Eukaryota*; *Opisthokonta*; *Metazoa*; *Eumetazoa*; *Bilateria*; *Protostomia*; *Lophotrochozoa*; *Mollusca*; *Bivalvia*; *Pteriomorphia*; *Ostreoida*; *Ostreoidea*; *Ostreidae*; *Crassostrea*"). For each gene, we thus computed the average proportion of its taxonomy units shared with its phylogenetic neighbors. This score was further normalized by the average value in the neighbors. The resulting taxonomy consistency score approaches 1.0 for nodes whose position in the protein tree is consistent with the species tree, and it is lower for putative contaminant sequences; we thus filtered out 64 genes with a taxonomy consistency score below 0.75. The second step of our phylogenetic filter was motivated by the presence of partial gene sequences (fragments), which we attributed to the imperfect quality of genomes and transcriptomes. These predictions can be readily detected by inspecting the sequence length across the protein tree: fragments are isolated cases with shorter lengths compared to their phylogenetic neighbors. We thus computed a length consistency score per prediction, defined as its CDS length divided by the average length of its 10 phylogenetic neighbors. We thus filtered out 474 genes with a score below 0.75 (i.e., those at least 25% shorter than their most similar sequences). Lastly, we also filtered out 139 predictions with pseudogene features (frameshifts or in-frame stops other than UGA) and 299 predictions without a (non-UGA) stop codon downstream (mostly in short transcriptomic fragments). Our final bona-fide set consisted of 1228 *SelenoP* predictions. The N-terminal protein tree, cleared of filtered out predictions, is shown in Supplementary Fig. 1.

Homology and modularity in SelenoP sequences

We set up a computational procedure to detect local homology both inter- and intra-sequences. We initially attempted to use Blastp v2.2.26 with permissive parameters (word size 2, max evalue 1000, query filtering turned off), but we realized that its algorithm by design does not allow detection of intra-sequence matches, thus precluding investigation of modularity. We finally employed Exonerate v2.4.0, run in "affine:-local" mode with permissive parameters (score threshold 30, word length 2), which instead returns both inter- and intra-sequence matches (Supplementary Fig. 3A). Exonerate assigns a score to each match, but it does not provide measures of statistical significance (e.g., *e*-values). We thus ran both programs on the protein sequences of the representatives of all phylogenetic clusters, in all-against-all fashion. We exploited the presence of many identical alignments in the outputs of Exonerate and Blast to calibrate an "Exonerate score to log *e*-value" ratio, thus allowing to assign "inferred *e*-values" to Exonerate hits (Supplementary Fig. 3B). We considered all Exonerate matches with 'inferred *e*-value < 0.01, and we visualized them with R as dot-matrix-like plots (Fig. 3). While we inspected results of all sequences, to reduce the complexity of plots, we finally decided to represent only a subset of all sequence representatives per phylogenetic cluster, removing those providing redundant information (e.g., a single representative for arachnid SelenoP was retained).

SECIS prediction and phylogeny

We used the program SECISearch3 [93] to detect potential SECIS elements in *SelenoP* sequences. We considered regions of 3000 nucleotides downstream of each CDS (or shorter if reaching over the contig end), and we scanned them using all three methods implemented in SECISearch3. During our complex filtering procedure (explained above), some gene predictions were combined to form consensus entries that were longer than their individual components. In those cases, we assigned to each new consensus entry the SECIS set with the highest number of predicted SECIS elements, among the ones in its merged components. To predict the phylogenetic tree of SECIS elements, we produced a structural alignment using the program Cmalign from the Infernal package v1.1.1, using the SECIS model at the core of SECISearch3 as template. Then, to reduce the number of sequences for phylogenetic reconstruction, we trimmed out the most abundant classes of genes: phylogenetic clusters vertebrate *SelenoP1* and vertebrate *SelenoP2*. We retained SECIS elements found in 40 genes selected randomly in each of these clusters and removed the rest from the alignment. We thus ran phylogenetic reconstruction using ETE3 [91] with "pmodeltest_soft_ultrafast" for evolutionary model selection and "phyml_default_bootstrap" for tree reconstruction. The resulting tree is shown in Supplementary Fig. 11.

Tetraselmis sp. algal culture

For oyster feed, we cultured *Tetraselmis* sp. algae using artificial sea water made with Instant Ocean

Aquarium sea salts adjusted to a salinity of 35 ppt. Algae were diluted in 80 mL of algae media (80% artificial sea water and 20% F2 Guillards media (Sigma G0154), either supplemented or not with 5 mg/L of sodium selenite (28.9 μM) (Sigma-214,485) diluted in artificial sea water. Algae were grown for 3 days with constant oxygenation and a 12-h light/dark cycle to allow Se incorporation. On the day of feeding, algal cells were equalized by counting cell numbers and equal amounts were fed to each corresponding oyster tank weekly for 6 weeks.

Aquaculture, selenium supplementation, and histology of *M. gigas*

Twenty diploid, 2-year-old Pacific oysters obtained from an oyster cultivation farm in Co. Clare, Ireland, were distributed equally into two tanks containing artificial seawater with salinity adjusted to 25 ppt and kept at constant temperature 16 °C. Denitrifying bacteria were added to aid in acclimation and break down of toxic waste. Twenty-four hours after feeding (to allow complete filtering of algal feed), oyster tissues were cross sectioned and prepared for histology for gonad development and sex determination.

Cross sections of diploid oysters were fixed in 90% fixative (Davidson Solution-Sigma) and 10% acetic acid for 24–48 h, dehydrated through graduated ethanol dilutions, and paraffin-wax embedded. Seven-micrometer-thick sections were cut and stained with hematoxylin–eosin. The slides were analyzed using a Nikon Eclipse 80i microscope with a 40× objective, and images were captured with a Nikon DXM 1200-C camera and processed using Andor IQ acquisition software (Andor Technology Ltd. Belfast, Northern Ireland). Sex and gonad development stage were analyzed using previously published criteria [94,95]. Only male oysters with developed gonads were subjected to total selenium determination and ribosome profiling library preparation.

ICP-MS: total selenium

Whole-body male oyster tissues were prepared for ICP-MS analysis by liquid nitrogen grinding. Independently, the algae-feed, tank water, and oyster cytoplasmic extract preparations were also analyzed. DigiPrep (SCP Science, Courtaboeuf, France) was used to heat the sample during acid digestion. The samples were weighed and left overnight in 0.2 to 0.5 mL of HNO_3 (depending on quantity of the sample available). One microliters of H_2O_2 was added, and the sample was digested in a DigiPrep (the digestion program: 0–30 min at room temperature, 30–240 min at 65 °C). The digests were diluted to reach the HNO_3 concentration of 4% and analyzed by ICP MS using the conditions optimized daily (nebulizer gas flow, RF power, lens voltage, and collision gas flow) [96]. We carried out external calibration at six levels, adding selenium to a blank sample (mixture of nitric acid, hydrogen peroxide, and water) to reach Se concentrations of 0.25, 0.5, 1, 2.5, 5, and 10 ppm. The ICP MS instrument used was an Agilent 7700 (Tokyo, Japan) fitted with a collision cell and a Meinhard nebulizer (Glass Expansion, Romainmotier, Switzerland).

Ribosome profiling and RNA sequencing library preparation

For ribosome profiling, soft tissues from two individual whole oysters, with similar determined levels of selenium from each supplementation group, were flash-frozen in liquid nitrogen and subsequently pulverized by grinding using a ceramic pestle and mortar, pooled, and lysed in 2 mL polysome lysis buffer [10 mM Tris–HCl (pH 7.5), 150 mM NaCl, 15 mM $MgCl_2$, 1% sodium deoxycholate, 1% Triton X100, 100 μg/mL cycloheximide, 2 mM DTT, and 2 μL Superase·IN RNase inhibitor]. Lysates were centrifuged at 16,000*g* for 10 min at 4 °C. One milliliter of supernatant was treated with 100 U of RNAse I at 25 °C for 45 min. RNAse I was deactivated with Superase·In at 65 °C for 5 min. Monosome fractions were isolated by loading RNAse I-treated lysates on a 10%–60% continuous sucrose gradient and centrifuged at 35,000 RPM for 3 h at 4 °C in a SW41Ti rotor in a Beckman ultracentrifuge. Gradients were chased with cesium chloride, and fractions containing the monosomes were identified by OD reading at a wavelength of 256 nm. RPFs were isolated from tightly defined monosome fractions by TRIzol extraction.

For RNA sequencing, polyA mRNA were isolated from the same samples using the Poly(A) Purist Mag kit (Ambion) and randomly fragmented using alkaline fragmentation buffer (2 mM EDTA, 10 mM Na_2CO_3, 90 mM $NaHCO_3$). Both RPFs and randomly fragmented PolyA were prepared following Ingolia's ribosome profiling library preparation protocol [97], omitting the experimental ribosomal RNA depletion step. The prepared cDNA libraries were sequenced by BGI Genomics Co., Ltd. Shenzhen, China (www.bgi.com). The samples were pooled in one SE50 multiplex lane where 3GB of data were allocated for each ribosome profiling sample and 0.6 GB were allocated for each RNA-sequencing sample.

Bioinformatic analysis of RNA-seq and riboseq

Using Ribogalaxy [98], raw sequencing reads were pre-processed before alignment to the transcriptome. Oyster ribosomal RNA sequences 5.8S (ENSRNA022717831), 5S (ENSRNA02271792), 28S (AB102757.1), and 18S (ENSRNA022718259) were identified *in silico* using Bowtie version 1.1.1

[99] and removed. The remaining reads were mapped with Bowtie to the oyster transcriptome [61] using the same parameters as trips-viz [100]. Metagene analysis was performed to assess triplet periodicity and P-site offset as a quality control (Supplementary Note 8). For metagene analysis, start and stop codons in each transcript were obtained from the transcriptome assembly ORF annotation [61]. Previously, we had identified transcripts corresponding to selenoproteins using Selenoprofiles [88] and manually selected a single transcript as a representative for each selenoprotein gene (Supplementary Table 1). Read counts per selenoprotein gene were normalized by transcript length (kbp) per million mapped reads (RPKMs and RPFKMs, for RNA-seq and riboseq respectively) using the programs cuffquant and cuffnorm from the package cufflinks version 2.2.1 [101]. Genes with RPKM or RPFKM below 1.0 in either selenium supplementation group (*DIO.2*, *SELENOH.1*, *PSTK.2*, *SBP2.117*) were discarded to avoid over interpretation in the differential expression analysis due to low coverage. Translation efficiency was computed as the ratio of RPFKM/RPKM for each gene. To calculate Sec URE [67,69], we defined the 5′ and 3′ regions for each selenoprotein CDS based on the position of the Sec-UGA codon (UGA1 in case of *SelenoP*). URE was expressed as the ratio of RPF density in the region 3′ of UGA to the region 5′ of UGA (3′RPFKM/5′RPFKM). Reads within 15 nt from AUG and 5 nt from stop codon were omitted to remove bias introduced by cycloheximide treatment. URE was not computed for selenoprotein genes in which the UGA codon was located near the 3′ end of the CDS (*SELENOK.1*, *SELENOO.2*, *SELENOS.1*, *TR.1*, *TR.2*) or near the AUG start (*DSBA.1*, *MSRA.2*, *SELENOW.1*, *SELENOW.2*). Aligned RNA-seq and riboseq reads were visualized with trips-viz for each individual selenoprotein mRNA, and plots were generated to compare supplemented and non-supplemented samples. Mapping of ambiguous reads were allowed for genes with more than one transcript isoform in the transcriptome. Minimum and maximum fragment length were set at 25 to 35 nt, respectively, for trips-viz visualization, corresponding to the expected size of the RPFs during translation.

In vivo ^{75}Se labeling of oyster larvae

Free-swimming larvae at 7-day and 14-day-old stages were gifts from an oyster cultivation facility (Pacific Sea Foods, Quilcene WA, USA). Additional larvae were obtained from the Rutgers Haskin Shellfish laboratory for method development. After 24-h acclimation in 10 L of artificial sea water and initial feeding with Instant Shellfish Diet1800, 100–200 oyster larvae (100 μm in size) were transferred into a 12-well plate with artificial sea water spiked with 1 μL of 100 μM ^{75}Se diluted in 1% DMSO for metabolic selenium incorporation. After 24 h, oyster larvae were washed, harvested, and mechanically lysed in RIP-A lysis buffer [50 mM Tris–HCl (pH 8.0), Triton X-100, 150 mM NaCl, 0.5% sodium deoxycholate, and protease inhibitors]. Protein extracts were electrophoresed in 10% SDS-PAGE, fixed, dried, and exposed to a Phosphorimager screen. Parallel Western blot probing was performed using SelenoP custom antibodies.

Immunoblot and densitometry

Custom antibodies, anti-NT SelenoP against oyster SelenoP N-terminal region before Sec-UGA 1 (immunogenic peptide TADGTDPVKARVN), and anti-CT SelenoP against the C-terminal region after Sec-UGA 43 (immunogenic peptide YCRTGTYDDRAH) were obtained from Genscript. These antibodies were tested for affinity and specificity (Supplementary Fig. 10). Immunoblot analysis using SelenoP custom antibodies were performed on oyster lysates used in ribosome profiling analysis. Two of the same samples (replicate = 2) were equalized to 50 μg of protein per lane, resolved on 12% SDS PAGE, and transferred to nitrocellulose membrane (Protran). The membrane was blocked with 5% milk in phosphate buffer saline–Tween20 (0.5% PBS-T) overnight in 4 °C and probed with 1:2500 dilutions of rabbit primary antibodies (anti-NT-SelenoP and anti-CT-SelenoP) in 5% milk–PBS-T for 1 h at RT. The membrane was washed three times with PBS-T. Immunoreactive bands were detected with appropriate fluorescently labeled secondary antibodies and scanned using LI-COR Odyssey® Infrared Imaging Scanner (LI-COR Biosciences). Full-length band intensity was quantified across samples using Image Lite Studio. Values were normalized against Ponceau S loading control and plotted as an average of two technical replicates.

SelenoP plasmid construction and oyster mutant generation

Native cDNA sequences were used to obtain gene blocks (DNA fragments) from Integrated DNA Technologies. An exception was made for the sequence of spider *P. tepidariorum*, obtained instead through gene synthesis (GenScript), due to its sequence complexity hindering gene-block generation. All *SelenoP* gene-block constructs were cloned into the pcDNA3.1 TOPO-TA vector cleaved by BamHI and AgeI-HF.

The plasmid with zebrafish *SelenoP* cDNA [51] was used as positive control. Mutant constructs were generated by either PCR or site directed mutagenesis. The Kozak context was added by Quick Change II kit (Agilent Technologies) site-directed

mutagenesis following the manufacturer's protocol and with primer sequences indicated in Supplementary Table 5. Mutants of the oyster *SelenoP* mRNA (Supplementary Fig. 5) were generated as follows. Del. 5′UTR mutant (Results) was generated by PCR amplification of native oyster sequence with primers indicated and cloned into double-digested pCDNA3.1 TOPO-TA vector. Syn. ISL mutants were introduced through PCR in three steps. Removal of sequence encoding the C-terminal Sec-rich domain (Del. C-Term mutant) was carried out by a two-step cloning procedure where the CDS was re-ligated with its 3′UTR after UGA 11−46 removal by PCR. Addition of oyster SECIS elements to zebrafish coding region was via Pac1 and Not1 double digest removal of zebrafish SECIS 1 and re-ligation of oyster SECIS amplified by PCR including restriction sites. Oyster SECIS element sequences were subcloned into the pcDNA3.1 TOPO-TA vector containing zebrafish CDS insert (mutants: Fus. 3′UTR, Fus. SECIS 1, and Fus SECIS 2). All restriction enzymes used for each insert are indicated in Table S5. Inserts digested with BglII/Age1-HF were inserted into a BamH1/Age1HF cut pCDNA 3.1 TOPO-TA vector, while the same restriction enzymes were used to cut the vector for all the other mutants. Subsequent ligation, transformation, and positive colony selection were by standard procedures. Plasmid DNA was purified using GeneJET Mini-Prep Plasmid Isolation Kit (Thermo Fisher). DNA sequencing was by Eurofins, Germany.

In vitro transcription, RRL translation, and ^{75}Se labeling

All cloned plasmid constructs were linearized by a single restriction enzyme digestion, *in vitro* transcribed by T7 polymerase and capped using mMessege mMachine kit (Ambion). A 110-nt vector sequence is present between the T7 promoter and the respective construct sequence. RRL (Promega) reactions were reconstituted with rat CT-SECISBP2 or oyster SECISBP2 and radiolabeled with ^{75}Se as described [50]. RRL reactions were denatured in sample buffer at 95 °C for 5 min and electrophoresed on 10% or 15% SDS-PAGE. The gel was fixed, dried, and exposed for autoradiography.

Oyster SECISBP2 recombinant protein purification

Full-length oyster *SECISBP2* (*FLSBP2*) CDS trimmed with Xba1 and Sac1HF digestion was cloned into bacterial vector (Pj307) [102] cleaved with Spe1 and Sac1HF. The ampicillin-resistant empty vector encodes an N-terminal Glutathione Sepharose Transferase (GST) tag followed by sequence specifying an HRV-3C protease cleavage site and a 6XHis-tag. A clone containing the *FLSBP2* insert was transformed into BL21 competent *Escherichia coli*. A selected colony was grown in 5 mL of LB-AMP media. Cells were then transferred to 3 L of LB-AMP media, grown at 37 °C for 2 h and on reaching OD_{600} of 0.6 induced with 0.05 mM IPTG, and grown overnight at 15 °C. Cells were centrifuged (5000 *g*, 10 min), washed with PBS, and lysed in a lysozyme-containing lysis buffer. Lysates were sonicated, centrifuged, and incubated overnight with GST beads (GE Healthcare Sigma 17-0756-01) at 4 °C. The GST beads were then washed three times [50 mM Tris−HCl (pH 8), 150 mM NaCl, 0.1% NP-40] and finally with 10 bead volumes of protease cleavage buffer [50 mM Tris−HCl (pH 8), 150 mM NaCl, 0.1% NP-40, 1 mM DTT, and 1 mM EDTA]. GST beads were then resuspended in 1 bead volume of cleavage buffer and 40 μL PreScission Protease (GE Healthcare, 27-0843-01) to cleave off the GST-tag. Concentration ensued in Amicon ultra-centrifugal filter units with 30-kDa molecular-weight-cutoff concentrators (Sigma). Following gel filtration using a Superdex-200 column, the buffer was substituted with PBS. An aliquot was subjected to SDS-PAGE and analyzed with Coomassie staining and Western blot.

RT-PCR and sequencing

E. complanata mussels were a gift from Department of Natural Resources, C-2 Annapolis, MD, USA. Total RNA was isolated from their tissue using Trizol (Invitrogen™). Reverse transcription (RT) was performed with oligo dT primer using SuperScript® III First-Strand Synthesis System (Invitrogen). PCR on the resulting cDNA was with Phusion polymerase (NEB) using the forward primer 5′ TAAACTGGCTGAGCCGCGGTGGCTC3′ and reverse primers 5′ ATATATAATATGCTAAGAGTGATCA 3′ (T1) and 5′ AAGTGACAAAACGCACAAGCAATGTTAAAATGCAC 3′ (T2). Amplified PCR product was gel purified by Zymoresearch DNA isolation kit as per manual and sent for Sanger sequencing using the following forward sequencing primers: 5′ TTGCATTCCCTGCTTTTGACATACTGTCG 3′ (S1), 5′ ACGTTGATTTTTGATGACGTCACTCAGAT 3′ (S2) and 5′ TCCATTTGATGAAAGAAAGCTAAAGAA3′ (S3).

Supplementary data to this article can be found online at https://doi.org/10.1016/j.jmb.2019.08.007.

CRediT authorship contribution statement

Janinah Baclaocos: Data curation, Investigation, Visualization, Writing - original draft, Methodology.- **Didac Santesmasses:** Data curation, Investigation, Visualization, Writing - original draft, Methodology. **Marco Mariotti:** Conceptualization, Data curation,

Investigation, Visualization, Writing - original draft, Methodology. **Katarzyna Bierła:** Methodology, Investigation, Writing - review & editing. **Michael B. Vetick:** Methodology, Investigation, Writing - review & editing. **Sharon Lynch:** Methodology, Investigation, Writing - review & editing. **Rob McAllen:** Methodology, Investigation, Writing - review & editing. **John J. Mackrill:** Methodology, Investigation, Writing - review & editing. **Gary Loughran:** Methodology, Investigation, Writing - review & editing. **Roderic Guigó:** Supervision, Writing - review & editing. **Joanna Szpunar:** Methodology, Investigation, Writing - review & editing. **Paul R. Copeland:** Supervision, Writing - review & editing. **Vadim N. Gladyshev:** Supervision, Writing - review & editing. **John F. Atkins:** Conceptualization, Supervision, Writing - original draft.

Acknowledgments

We thank Sumangala Shetty and Mark Pinkerton for advice; Iarfhlaith Connellan from Cartron Point Shellfish Ltd., Co.; Clare for providing the diploid oysters and microalgae; Lizzie Nelson of Pacific Sea Foods, Quilcene, Washington, for a gift of oyster larvae; Matt Ashton of Department of Natural Resources, Maryland, for a gift *Elliptio complanata* fresh water mussels; Declan O'Sullivan of Collorus, Co. Kerry, Ireland, for provision of marine farmed *Mytilus edulis* mussels; and Ximing Guo, for oyster larvae from the Rutgers Haskin Shellfish Laboratory. M.M. was supported by EMBO short-term fellowship ASTF 289-2014. The work was supported by the following grants: NIH DK117149, GM065204, and AG021518 (V.N.G.); BIO2014-57291-R from the Spanish Ministry of Economy and Competitiveness (R.G.), NIH GM077073 (P.R.C.), Science Foundation Ireland (13/IA/1853), and Irish Research Council (IRCLA/2019/74 n) (J.F.A).

Received 29 May 2019;
Received in revised form 5 August 2019;
Accepted 11 August 2019
Available online 20 August 2019

Keywords:
selenoprotein;
selenocysteine;
recoding;
dynamic redefinition;
evolution

†Joint first authors.

Abbreviations used:
Sec, selenocysteine; SECIS, *se*lenocysteine *i*nsertion *se*quence; SRE, Sec redefinition element; SelenoP, selenoprotein P; ISL, initiation stem loop; Cys, cysteine; CDS, coding sequence; RRL, rabbit reticulocyte lysate; ORF, open reading frame; RPF, ribosome-protected fragment; NMD, nonsense-mediated decay; ICP-MS, inductively coupled mass spectrometry; URE, UGA-redefinition efficiency; GST, Glutathione Sepharose Transferase.

References

[1] V.M. Labunskyy, D.L. Hatfield, V.N. Gladyshev, Selenoproteins: molecular pathways and physiological roles, Physiol. Rev. 94 (2014) 739–777, https://doi.org/10.1152/physrev.00039.2013.

[2] M.J. Maroney, R.J. Hondal, Selenium versus sulfur: reversibility of chemical reactions and resistance to permanent oxidation in proteins and nucleic acids, Free Radic. Biol. Med. 127 (2018) 228–237, https://doi.org/10.1016/j.freeradbiomed.2018.03.035.

[3] I. Ingold, C. Berndt, S. Schmitt, S. Doll, G. Poschmann, K. Buday, A. Roveri, X. Peng, F. Porto Freitas, T. Seibt, L. Mehr, M. Aichler, A. Walch, D. Lamp, M. Jastroch, S. Miyamoto, W. Wurst, F. Ursini, E.S.J. Arnér, N. Fradejas-Villar, U. Schweizer, H. Zischka, J.P. Friedmann Angeli, M. Conrad, Selenium utilization by GPX4 is required to prevent hydroperoxide-induced ferroptosis, Cell. 172 (2018) 409–422.e21. https://doi.org/10.1016/j.cell.2017.11.048.

[4] R.F. Burk, K.E. Hill, Regulation of selenium metabolism and transport, Annu. Rev. Nutr. 35 (2015) 109–134, https://doi.org/10.1146/annurev-nutr-071714-034250.

[5] U. Schweizer, N. Fradejas-Villar, Why 21? The significance of selenoproteins for human health revealed by inborn errors of metabolism, FASEB J. 30 (2016) 3669–3681, https://doi.org/10.1096/fj.201600424.

[6] Y.M. Xia, K.E. Hill, R.F. Burk, Biochemical studies of a selenium-deficient population in China: measurement of selenium, glutathione peroxidase and other oxidant defense indices in blood, J. Nutr. 119 (1989) 1318–1326, https://doi.org/10.1093/jn/119.9.1318.

[7] M.L. Jackson, Selenium: geochemical distribution and associations with human heart and cancer death rates and longevity in China and the United States., Biol. Trace Elem. Res. 15 (n.d.) 13–21. http://www.ncbi.nlm.nih.gov/pubmed/2484511 (accessed July 25, 2019).

[8] J.A. Long, R.R. Large, M.S.Y. Lee, M.J. Benton, L.V. Danyushevsky, L.M. Chiappe, J.A. Halpin, D. Cantrill, B. Lottermoser, Severe selenium depletion in the Phanerozoic oceans as a factor in three global mass extinction events, Gondwana Res. 36 (2016) 209–218, https://doi.org/10.1016/j.gr.2015.10.001.

[9] A. Böck, K. Forchhammer, J. Heider, W. Leinfelder, G. Sawers, B. Veprek, F. Zinoni, Selenocysteine: the 21st amino acid, Mol. Microbiol. 5 (1991) 515–520. http://www.ncbi.nlm.nih.gov/pubmed/1828528. (Accessed 19 August 2013).

[10] J.F. Atkins, R.F. Gesteland, The twenty-first amino acid., Nature. 407 (2000) 463, 465. https://doi.org/10.1038/35035189.

[11] T. Mukai, M. Englert, H.J. Tripp, C. Miller, N.N. Ivanova, E.M. Rubin, N.C. Kyrpides, D. Söll, Facile recoding of

selenocysteine in nature, Angew. Chemie Int. Ed. 55 (2016) 5337–5341, https://doi.org/10.1002/anie.201511657.
[12] M.J. Berry, L. Banu, Y. Chen, S.J. Mandel, J.D. Kieffer, J.W. Harney, P.R. Larsen, Recognition of UGA as a selenocysteine codon in type I deiodinase requires sequences in the 3′ untranslated region, Nature. 353 (1991) 273–276. http://www.nature.com/nature/journal/v353/n6341/abs/353273a0.html.
[13] M.J. Berry, L. Banu, J.W. Harney, P.R. Larsen, Functional characterization of the eukaryotic SECIS elements which direct selenocysteine insertion at UGA codons, EMBO J. 12 (1993) 3315–3322. http://www.pubmedcentral.nih.gov/articlerender.fcgi?artid=413599&tool=pmcentrez&rendertype=abstract. (Accessed 13 July 2014).
[14] R. Walczak, P. Carbon, A. Krol, An essential non-Watson–-Crick base pair motif in 3′UTR to mediate selenoprotein translation, RNA. 4 (1998) 74–84. http://www.ncbi.nlm.nih.gov/pubmed/9436910. (Accessed 25 July 2019).
[15] E. Grundner-Culemann, G.W. Martin, J.W. Harney, M.J. Berry, Two distinct SECIS structures capable of directing selenocysteine incorporation in eukaryotes, RNA. 5 (1999) 625–635. http://www.pubmedcentral.nih.gov/articlerender.fcgi?artid=1369790&tool=pmcentrez&rendertype=abstract.
[16] P.R. Copeland, J.E. Fletcher, B.A. Carlson, D.L. Hatfield, D.M. Driscoll, A novel RNA binding protein, SBP2, is required for the translation of mammalian selenoprotein mRNAs, EMBO J. 19 (2000) 306–314, https://doi.org/10.1093/emboj/19.2.306.
[17] L. Chavatte, B.A. Brown, D.M. Driscoll, Ribosomal protein L30 is a component of the UGA-selenocysteine recoding machinery in eukaryotes, Nat. Struct. Mol. Biol. 12 (2005) 408–416. http://www.nature.com/nsmb/journal/v12/n5/abs/nsmb922.html.
[18] J.L. Bubenik, A.C. Miniard, D.M. Driscoll, Characterization of the UGA-recoding and SECIS-binding activities of SECIS-binding protein 2, RNA Biol. 11 (2014) 1402–1413, https://doi.org/10.1080/15476286.2014.996472.
[19] D. Fagegaltier, N. Hubert, K. Yamada, T. Mizutani, P. Carbon, A. Krol, Characterization of mSelB, a novel mammalian elongation factor for selenoprotein translation, EMBO J. 19 (2000) 4796–4805, https://doi.org/10.1093/emboj/19.17.4796.
[20] R.M. Tujebajeva, P.R. Copeland, X.M. Xu, B.A. Carlson, J.W. Harney, D.M. Driscoll, D.L. Hatfield, M.J. Berry, Decoding apparatus for eukaryotic selenocysteine insertion, EMBO Rep. 1 (2000) 158–163, https://doi.org/10.1038/sj.embor.embor604.
[21] A.M. Zavacki, J.B. Mansell, M. Chung, B. Klimovitsky, J.W. Harney, M.J. Berry, Coupled tRNA(Sec)-dependent assembly of the selenocysteine decoding apparatus, Mol. Cell 11 (2003) 773–781. http://www.ncbi.nlm.nih.gov/pubmed/12667458. (Accessed 4 July 2014).
[22] J. Donovan, K. Caban, R. Ranaweera, J.N. Gonzalez-Flores, P.R. Copeland, A novel protein domain induces high affinity selenocysteine insertion sequence binding and elongation factor recruitment, J. Biol. Chem. 283 (2008) 35129. http://www.jbc.org/cgi/content/abstract/283/50/35129.
[23] B.A. Carlson, M.-H. Yoo, P.A. Tsuji, V.N. Gladyshev, D.L. Hatfield, Mouse models targeting selenocysteine tRNA expression for elucidating the role of selenoproteins in health and development, Molecules. 14 (2009) 3509–3527, https://doi.org/10.3390/molecules14093509.
[24] M.E. Budiman, J.L. Bubenik, A.C. Miniard, L.M. Middleton, C.A. Gerber, A. Cash, D.M. Driscoll, Eukaryotic initiation factor 4a3 is a selenium-regulated RNA-binding protein that selectively inhibits selenocysteine incorporation, Mol. Cell 35 (2009) 479–489, https://doi.org/10.1016/j.molcel.2009.06.026.
[25] A.C. Miniard, L.M. Middleton, M.E. Budiman, C.A. Gerber, D.M. Driscoll, Nucleolin binds to a subset of selenoprotein mRNAs and regulates their expression., Nucleic Acids Res. (2010). https://doi.org/10.1093/nar/gkq247.
[26] M.T. Howard, G. Aggarwal, C.B. Anderson, S. Khatri, K.M. Flanigan, J.F. Atkins, Recoding elements located adjacent to a subset of eukaryal selenocysteine-specifying UGA codons, EMBO J. 24 (2005) 1596–1607, https://doi.org/10.1038/sj.emboj.7600642.
[27] M.T. Howard, M.W. Moyle, G. Aggarwal, B.A. Carlson, C.B. Anderson, A recoding element that stimulates decoding of UGA codons by sec tRNA[Ser]Sec, RNA. 13 (2007) 912–920, https://doi.org/10.1261/rna.473907.
[28] B. Maiti, S. Arbogast, V. Allamand, M.W. Moyle, C.B. Anderson, P. Richard, P. Guicheney, A. Ferreiro, K.M. Flanigan, M.T. Howard, A mutation in the SEPN1 selenocysteine redefinition element (SRE) reduces selenocysteine incorporation and leads to SEPN1-related myopathy, Hum. Mutat. 30 (2009) 411–416, https://doi.org/10.1002/humu.20879.
[29] J.L. Bubenik, A.C. Miniard, D.M. Driscoll, Alternative transcripts and 3′UTR elements govern the incorporation of selenocysteine into selenoprotein S, PLoS One 8 (2013), e62102, https://doi.org/10.1371/journal.pone.0062102.
[30] V.N. Gladyshev, E.S. Arnér, M.J. Berry, R. Brigelius-Flohé, E.A. Bruford, R.F. Burk, B.A. Carlson, S. Castellano, L. Chavatte, M. Conrad, P.R. Copeland, A.M. Diamond, D.M. Driscoll, A. Ferreiro, L. Flohé, F.R. Green, R. Guigó, D.E. Handy, D.L. Hatfield, J. Hesketh, P.R. Hoffmann, A. Holmgren, R.J. Hondal, M.T. Howard, K. Huang, H.-Y. Kim, I.Y. Kim, J. Köhrle, A. Krol, G. V Kryukov, B.J. Lee, B.C. Lee, X.G. Lei, Q. Liu, A. Lescure, A.V. Lobanov, J. Loscalzo, M. Maiorino, M. Mariotti, K.S. Prabhu, M.P. Rayman, S. Rozovsky, G. Salinas, E.E. Schmidt, L. Schomburg, U. Schweizer, M. Simonović, R.A. Sunde, P.A. Tsuji, S. Tweedie, F. Ursini, P.D. Whanger, Y. Zhang, Selenoprotein gene nomenclature., J. Biol. Chem. (2016). https://doi.org/10.1074/jbc.M116.756155.
[31] G. Kryukov, V. Gladyshev, Selenium metabolism in zebrafish: multiplicity of selenoprotein genes and expression of a protein containing 17 selenocysteine residues, Genes Cells 5 (2000) 1049. http://www.genestocellsonline.org/cgi/content/abstract/5/12/1049.
[32] S. Kurokawa, S. Eriksson, K.L. Rose, S. Wu, A.K. Motley, S. Hill, V.P. Winfrey, W.H. McDonald, M.R. Capecchi, J.F. Atkins, E.S.J. Arnér, K.E. Hill, R.F. Burk, Sepp1(UF) forms are N-terminal selenoprotein P truncations that have peroxidase activity when coupled with thioredoxin reductase-1, Free Radic. Biol. Med. 69 (2014) 67–76, https://doi.org/10.1016/j.freeradbiomed.2014.01.010.
[33] A.V. Lobanov, D.L. Hatfield, V.N. Gladyshev, Reduced reliance on the trace element selenium during evolution of mammals., Genome Biol. 9 (2008) R62. https://doi.org/10.1186/gb-2008-9-3-r62.
[34] K.E. Hill, R.S. Lloyd, J.G. Yang, R. Read, R.F. Burk, The cDNA for rat selenoprotein P contains 10 TGA codons in the open reading frame, J. Biol. Chem. 266 (1991) 10050–10053. http://www.ncbi.nlm.nih.gov/pubmed/2037562. (Accessed 25 July 2019).

[35] S. Himeno, H.S. Chittum, R.F. Burk, Isoforms of selenoprotein P in rat plasma, J. Biol. Chem. 271 (1996) 15769–15775, https://doi.org/10.1074/jbc.271.26.15769.
[36] S. Ma, K.E. Hill, R.M. Caprioli, R.F. Burk, Mass spectrometric characterization of full-length rat selenoprotein P and three isoforms shortened at the C terminus. Evidence that three UGA codons in the mRNA open reading frame have alternative functions of specifying selenocysteine insertion or translation termination., J. Biol. Chem. 277 (2002) 12749–54. https://doi.org/10.1074/jbc.M111462200.
[37] S. Wu, M. Mariotti, D. Santesmasses, K.E. Hill, J. Baclaocos, E. Aparicio-Prat, S. Li, J. Mackrill, Y. Wu, M.T. Howard, M. Capecchi, R. Guigó, R.F. Burk, J.F. Atkins, Human selenoprotein P and S variant mRNAs with different numbers of SECIS elements and inferences from mutant mice of the roles of multiple SECIS elements, Open Biol. 6 (2016) 160241, https://doi.org/10.1098/rsob.160241.
[38] A.V. Lobanov, D.E. Fomenko, Y. Zhang, A. Sengupta, D.L. Hatfield, V.N. Gladyshev, Evolutionary dynamics of eukaryotic selenoproteomes: large selenoproteomes may associate with aquatic life and small with terrestrial life., Genome Biol. 8 (2007) R198. https://doi.org/10.1186/gb-2007-8-9-r198.
[39] L. Jiang, J. Ni, Q. Liu, Evolution of selenoproteins in the metazoan, BMC Genomics 13 (2012) 446, https://doi.org/10.1186/1471-2164-13-446.
[40] K.E. Hill, R.S. Lloyd, R.F. Burk, Conserved nucleotide sequences in the open reading frame and 3′ untranslated region of selenoprotein P mRNA, Proc. Natl. Acad. Sci. U. S. A. 90 (1993) 537–541, https://doi.org/10.1073/pnas.90.2.537.
[41] M. Mariotti, S. Shetty, L. Baird, S. Wu, G. Loughran, P.R. Copeland, J.F. Atkins, M.T. Howard, Multiple RNA structures affect translation initiation and UGA redefinition efficiency during synthesis of selenoprotein P., Nucleic Acids Res. 45 (2017) 13004–13015. https://doi.org/10.1093/nar/gkx982.
[42] C.E. Chapple, R. Guigó, Relaxation of selective constraints causes independent selenoprotein extinction in insect genomes, PLoS One. 3 (2008).
[43] M. Mariotti, D. Santesmasses, S. Capella-Gutierrez, A. Mateo, C. Arnan, R. Johnson, S. D'Aniello, S.H. Yim, V.N. Gladyshev, F. Serras, M. Corominas, T. Gabaldón, R. Guigó, Evolution of selenophosphate synthetases: emergence and relocation of function through independent duplications and recurrent subfunctionalization, Genome Res. 25 (2015) 1256–1267, https://doi.org/10.1101/gr.190538.115.
[44] M. Mariotti, G. Salinas, T. Gabaldón, V.N. Gladyshev, Utilization of selenocysteine in early-branching fungal phyla, Nat. Microbiol. (2019), https://doi.org/10.1038/s41564-018-0354-9.
[45] M. Mariotti, P.G. Ridge, Y. Zhang, A.V. Lobanov, T.H. Pringle, R. Guigo, D.L. Hatfield, V.N. Gladyshev, Composition and evolution of the vertebrate and mammalian selenoproteomes., PLoS One. 7 (2012) e33066. https://doi.org/10.1371/journal.pone.0033066.
[46] P. Dehal, J.L. Boore, Two rounds of whole genome duplication in the ancestral vertebrate, PLoS Biol. 3 (2005), e314, https://doi.org/10.1371/journal.pbio.0030314.
[47] M. Mariotti, Selenocysteine extinctions in insects, in: C. Raman, M. Goldsmith, T. Agunbiade (Eds.), Short Views Insect Genomics Proteomics. Entomol. Focus vol. 4, Springer, Cham, 2016, pp. 113–140.
[48] A. Mehta, C.M. Rebsch, S.A. Kinzy, J.E. Fletcher, P.R. Copeland, Efficiency of mammalian selenocysteine incorporation, J. Biol. Chem. 279 (2004) 37852–37859, https://doi.org/10.1074/jbc.M404639200.
[49] L. Latrèche, O. Jean-Jean, D.M. Driscoll, L. Chavatte, Novel structural determinants in human SECIS elements modulate the translational recoding of UGA as selenocysteine, Nucleic Acids Res. 37 (2009) 5868–5880, https://doi.org/10.1093/nar/gkp635.
[50] S.P. Shetty, R. Shah, P.R. Copeland, Regulation of Selenocysteine incorporation into the selenium transport protein, selenoprotein P, J. Biol. Chem. 289 (2014) 25317–25326, https://doi.org/10.1074/jbc.M114.590430.
[51] S.P. Shetty, R. Sturts, M. Vetick, P.R. Copeland, Processive incorporation of multiple selenocysteine residues is driven by a novel feature of the selenocysteine insertion sequence, J. Biol. Chem. 293 (2018) 19377–19386, https://doi.org/10.1074/jbc.RA118.005211.
[52] D. Salvi, P. Mariottini, Molecular taxonomy in 2D: a novel ITS2 rRNA sequence-structure approach guides the description of the oysters' subfamily Saccostreinae and the genus Magallana (Bivalvia: Ostreidae), Zool. J. Linnean Soc. 179 (2016) 263–276, https://doi.org/10.1111/zoj.12455.
[53] M. Iacono, F. Mignone, G. Pesole, uAUG and uORFs in human and rodent 5′untranslated mRNAs, Gene. 349 (2005) 97–105, https://doi.org/10.1016/j.gene.2004.11.041.
[54] A. Churbanov, I.B. Rogozin, V.N. Babenko, H. Ali, E.V. Koonin, Evolutionary conservation suggests a regulatory function of AUG triplets in 5′-UTRs of eukaryotic genes., Nucleic Acids Res. 33 (2005) 5512–20. https://doi.org/10.1093/nar/gki847.
[55] A.G. Hinnebusch, I.P. Ivanov, N. Sonenberg, Translational control by 5′-untranslated regions of eukaryotic mRNAs, Science. 352 (2016) 1413–1416. https://doi.org/10.1126/science.aad9868.
[56] Z. Stoytcheva, R.M. Tujebajeva, J.W. Harney, M.J. Berry, Efficient incorporation of multiple selenocysteines involves an inefficient decoding step serving as a potential translational checkpoint and ribosome bottleneck, Mol. Cell. Biol. 26 (2006) 9177–9184, https://doi.org/10.1128/MCB.00856-06.
[57] S.M. Fixsen, M.T. Howard, Processive selenocysteine incorporation during synthesis of eukaryotic selenoproteins, J. Mol. Biol. 399 (2010) 385–396, https://doi.org/10.1016/j.jmb.2010.04.033.
[58] J. Donovan, P.R. Copeland, Evolutionary history of selenocysteine incorporation from the perspective of SECIS binding proteins, BMC Evol. Biol. 9 (2009) 229, https://doi.org/10.1186/1471-2148-9-229.
[59] J. Donovan, P.R. Copeland, Selenocysteine insertion sequence binding protein 2L is implicated as a novel post-transcriptional regulator of selenoprotein expression, PLoS One 7 (2012), e35581, https://doi.org/10.1371/journal.pone.0035581.
[60] G. Zhang, X. Fang, X. Guo, L. Li, R. Luo, F. Xu, P. Yang, L. Zhang, X. Wang, H. Qi, Z. Xiong, H. Que, Y. Xie, P.W.H. Holland, J. Paps, Y. Zhu, F. Wu, Y. Chen, J. Wang, C. Peng, J. Meng, L. Yang, J. Liu, B. Wen, N. Zhang, Z. Huang, Q. Zhu, Y. Feng, A. Mount, D. Hedgecock, Z. Xu, Y. Liu, T. Domazet-Lošo, Y. Du, X. Sun, S. Zhang, B. Liu, P. Cheng, X. Jiang, J. Li, D. Fan, W. Wang, W. Fu, T. Wang, B. Wang, J. Zhang, Z. Peng, Y. Li, N. Li, J. Wang, M. Chen, Y. He, F. Tan, X. Song, Q. Zheng, R. Huang, H. Yang, X. Du, L. Chen, M. Yang, P.M. Gaffney, S. Wang, L. Luo, Z. She, Y. Ming, W. Huang, S. Zhang, B. Huang, Y. Zhang, T.

Qu, P. Ni, G. Miao, J. Wang, Q. Wang, C.E.W. Steinberg, H. Wang, N. Li, L. Qian, G. Zhang, Y. Li, H. Yang, X. Liu, J. Wang, Y. Yin, J. Wang, The oyster genome reveals stress adaptation and complexity of shell formation., Nature. 490 (2012) 49–54. https://doi.org/10.1038/nature11413.

[61] G. Riviere, C. Klopp, N. Ibouniyamine, A. Huvet, P. Boudry, P. Favrel, GigaTON: an extensive publicly searchable database providing a new reference transcriptome in the pacific oyster Crassostrea gigas, BMC Bioinformatics. 16 (2015) 401, https://doi.org/10.1186/s12859-015-0833-4.

[62] Y. Zhang, D.E. Fomenko, V.N. Gladyshev, The microbial selenoproteome of the Sargasso Sea, Genome Biol. 6 (2005) R37, https://doi.org/10.1186/gb-2005-6-4-r37.

[63] C.J. Gobler, A.V. Lobanov, Y.-Z. Tang, A.A. Turanov, Y. Zhang, M. Doblin, G.T. Taylor, S.A. Sañudo-Wilhelmy, I.V. Grigoriev, V.N. Gladyshev, The central role of selenium in the biochemistry and ecology of the harmful pelagophyte, Aureococcus anophagefferens., ISME J. 7 (2013) 1333–43. https://doi.org/10.1038/ismej.2013.25.

[64] P.S. Rainbow, B.D. Smith, Trophic transfer of trace metals: subcellular compartmentalisation in bivalve prey and comparative assimilation efficiencies of two invertebrate predators, J. Exp. Mar. Bio. Ecol. 390 (2010) 143–148, https://doi.org/10.1016/J.JEMBE.2010.05.002.

[65] D. Umysová, M. Vítová, I. Dousková, K. Bisová, M. Hlavová, M. Cízková, J. Machát, J. Doucha, V. Zachleder, Bioaccumulation and toxicity of selenium compounds in the green alga Scenedesmus quadricauda, BMC Plant Biol. 9 (2009) 58, https://doi.org/10.1186/1471-2229-9-58.

[66] X. Sun, Y. Zhong, Z. Huang, Y. Yang, Selenium accumulation in unicellular green alga Chlorella vulgaris and its effects on antioxidant enzymes and content of photosynthetic pigments, PLoS One 9 (2014), e112270, https://doi.org/10.1371/journal.pone.0112270.

[67] M.T. Howard, B.A. Carlson, C.B. Anderson, D.L. Hatfield, Translational redefinition of UGA codons is regulated by selenium availability, J. Biol. Chem. 288 (2013) 19401–19413, https://doi.org/10.1074/jbc.M113.481051.

[68] P.A. Tsuji, B.A. Carlson, C.B. Anderson, H.E. Seifried, D.L. Hatfield, M.T. Howard, Dietary selenium levels affect selenoprotein expression and support the interferon-γ and IL-6 immune response pathways in mice., Nutrients. 7 (2015) 6529–49. https://doi.org/10.3390/nu7085297.

[69] N. Fradejas-Villar, S. Seeher, C.B. Anderson, M. Doengi, B.A. Carlson, D.L. Hatfield, U. Schweizer, M.T. Howard, The RNA-binding protein Secisbp2 differentially modulates UGA codon reassignment and RNA decay., Nucleic Acids Res. 45 (2017) 4094–4107. https://doi.org/10.1093/nar/gkw1255.

[70] A.A. Turanov, R.A. Everley, S. Hybsier, K. Renko, L. Schomburg, S.P. Gygi, D.L. Hatfield, V.N. Gladyshev, Regulation of Selenocysteine content of human selenoprotein P by dietary selenium and insertion of cysteine in place of selenocysteine, PLoS One 10 (2015), e0140353, https://doi.org/10.1371/journal.pone.0140353.

[71] Y. Xia, K.E. Hill, D.W. Byrne, J. Xu, R.F. Burk, Effectiveness of selenium supplements in a low-selenium area of China, Am. J. Clin. Nutr. 81 (2005) 829–834, https://doi.org/10.1093/ajcn/81.4.829.

[72] A.P. Kipp, D. Strohm, R. Brigelius-Flohé, L. Schomburg, A. Bechthold, E. Leschik-Bonnet, H. Heseker, German Nutrition Society (DGE), Revised reference values for selenium intake., J. Trace Elem. Med. Biol. 32 (2015) 195–9. https://doi.org/10.1016/j.jtemb.2015.07.005.

[73] G.K. Sarangi, F. Romagné, S. Castellano, Distinct patterns of selection in selenium-dependent genes between land and aquatic vertebrates, Mol. Biol. Evol. 35 (2018) 1744–1756, https://doi.org/10.1093/molbev/msy070.

[74] M.A. Bryszewska, A. Måge, Determination of selenium and its compounds in marine organisms, J. Trace Elem. Med. Biol. 29 (2015) 91–98, https://doi.org/10.1016/j.jtemb.2014.10.004.

[75] P.M. Moriarty, C.C. Reddy, L.E. Maquat, Selenium deficiency reduces the abundance of mRNA for se-dependent glutathione peroxidase 1 by a UGA-dependent mechanism likely to be nonsense codon-mediated decay of cytoplasmic mRNA, Mol. Cell. Biol. 18 (1998) 2932–2939, https://doi.org/10.1128/MCB.18.5.2932.

[76] R.A. Sunde, A.M. Raines, Selenium regulation of the selenoprotein and nonselenoprotein transcriptomes in rodents, Adv. Nutr. 2 (2011) 138–150, https://doi.org/10.3945/an.110.000240.

[77] Q.P. Gu, W. Ream, P.D. Whanger, Selenoprotein W gene regulation by selenium in L8 cells., Biometals. 15 (2002) 411–20. http://www.ncbi.nlm.nih.gov/pubmed/12405536 (accessed July 25, 2019).

[78] H.A. Spiller, Rethinking mercury: the role of selenium in the pathophysiology of mercury toxicity., Clin. Toxicol. (Phila). 56 (2018) 313–326. https://doi.org/10.1080/15563650.2017.1400555.

[79] L.H. Hedge, N.A. Knott, E.L. Johnston, Dredging related metal bioaccumulation in oysters, Mar. Pollut. Bull. 58 (2009) 832–840, https://doi.org/10.1016/j.marpolbul.2009.01.020.

[80] L. Schomburg, U. Schweizer, Hierarchical regulation of selenoprotein expression and sex-specific effects of selenium, BBA - Gen. Subj (2009), https://doi.org/10.1016/j.bbagen.2009.03.015.

[81] S. Kurokawa, M.J. Berry, Selenium. Role of the essential metalloid in health, Met. Ions Life Sci. 2013; 13:499–534. https://doi.org/10.1007/978-94-007-7500-8_16.

[82] J. Jagodnik, C. Chiaruttini, M. Guillier, Stem–loop structures within mRNA coding sequences activate translation initiation and mediate control by small regulatory RNAs., Mol. Cell. 68 (2017) 158–170.e3. https://doi.org/10.1016/j.molcel.2017.08.015.

[83] S. Seeher, U. Schweizer, Targeted deletion of Secisbp2 reduces, but does not abrogate, selenoprotein expression and leads to striatal interneuron loss, Free Radic. Biol. Med. 75 (2014) S9, https://doi.org/10.1016/j.freeradbiomed.2014.10.849.

[84] A.A. Turanov, A.V. Lobanov, D.E. Fomenko, H.G. Morrison, M.L. Sogin, L.A. Klobutcher, D.L. Hatfield, V.N. Gladyshev, Genetic code supports targeted insertion of two amino acids by one codon, Science. 323 (2009) 259. https://doi.org/10.1126/science.1164748.

[85] S.P. Shetty, P.R. Copeland, The selenium transport protein, selenoprotein P, requires coding sequence determinants to promote efficient selenocysteine incorporation, J. Mol. Biol. 430 (2018) 5217–5232, https://doi.org/10.1016/j.jmb.2018.09.005.

[86] M.E. Budiman, J.L. Bubenik, D.M. Driscoll, Identification of a signature motif for the eIF4a3–SECIS interaction, Nucleic Acids Res. 39 (2011) 7730–7739, https://doi.org/10.1093/nar/gkr446.

[87] J.F. Atkins, A. Bock, S. Matsufuji, R.F. Gesteland, Dynamics of the genetic code, in: R.F. Gesteland, T.R. Cech, J.F. Atkins (Eds.), RNA World, 2nd ed., Press, 1999: pp. 637–673.
[88] M. Mariotti, R. Guigó, Selenoprofiles: profile-based scanning of eukaryotic genome sequences for selenoprotein genes, Bioinformatics. 26 (2010) 2656–2663, https://doi.org/10.1093/bioinformatics/btq516.
[89] K.M. Kocot, T.H. Struck, J. Merkel, D.S. Waits, C. Todt, P.M. Brannock, D.A. Weese, J.T. Cannon, L.L. Moroz, B. Lieb, K.M. Halanych, Phylogenomics of lophotrochozoa with consideration of systematic error, Syst. Biol. 66 (2017) 256–282, https://doi.org/10.1093/sysbio/syw079.
[90] F. Sievers, D.G. Higgins, Clustal Omega for making accurate alignments of many protein sequences, Protein Sci. 27 (2018) 135–145, https://doi.org/10.1002/pro.3290.
[91] J. Huerta-Cepas, F. Serra, P. Bork, ETE 3: reconstruction, analysis, and visualization of phylogenomic data, Mol. Biol. Evol. 33 (2016) 1635–1638, https://doi.org/10.1093/molbev/msw046.
[92] A. Stamatakis, RAxML version 8: a tool for phylogenetic analysis and post-analysis of large phylogenies, Bioinformatics. 30 (2014) 1312–1313, https://doi.org/10.1093/bioinformatics/btu033.
[93] M. Mariotti, A.V. Lobanov, R. Guigo, V.N. Gladyshev, SECISearch3 and Seblastian: new tools for prediction of SECIS elements and selenoproteins., Nucleic Acids Res. 41 (2013) e149. https://doi.org/10.1093/nar/gkt550.
[94] A. Jouaux, C. Heude-Berthelin, P. Sourdaine, M. Mathieu, K. Kellner, Gametogenic stages in triploid oysters Crassostrea gigas: irregular locking of gonial proliferation and subsequent reproductive effort, J. Exp. Mar. Bio. Ecol. 395 (2010) 162–170, https://doi.org/10.1016/J.JEMBE.2010.08.030.
[95] Q. Li, W. Liu, K. Shirasu, W. Chen, S. Jiang, Reproductive cycle and biochemical composition of the Zhe oyster Crassostrea plicatula Gmelin in an eastern coastal bay of China, Aquaculture. 261 (2006) 752–759, https://doi.org/10.1016/J.AQUACULTURE.2006.08.023.
[96] Y. Ogra, K. Ishiwata, J. Ruiz Encinar, R. Łobiński, K.T. Suzuki, Speciation of selenium in selenium-enriched shiitake mushroom, Lentinula edodes, Anal. Bioanal. Chem. 379 (2004) 861–866, https://doi.org/10.1007/s00216-004-2670-6.
[97] N.T. Ingolia, G.A. Brar, S. Rouskin, A.M. McGeachy, J.S. Weissman, The ribosome profiling strategy for monitoring translation in vivo by deep sequencing of ribosome-protected mRNA fragments, Nat. Protoc. 7 (2012) 1534–1550, https://doi.org/10.1038/nprot.2012.086.
[98] A.M. Michel, J.P.A. Mullan, V. Velayudhan, P.B.F. O'Connor, C.A. Donohue, P.V. Baranov, RiboGalaxy: A browser based platform for the alignment, analysis and visualization of ribosome profiling data., RNA Biol. 13 (2016) 316–9. https://doi.org/10.1080/15476286.2016.1141862.
[99] B. Langmead, C. Trapnell, M. Pop, S.L. Salzberg, Ultrafast and memory-efficient alignment of short DNA sequences to the human genome, Genome Biol. 10 (2009) R25, https://doi.org/10.1186/gb-2009-10-3-r25.
[100] S.J. Kiniry, P.B.F. O'Connor, A.M. Michel, P.V. Baranov, Trips-Viz: a transcriptome browser for exploring Ribo-Seq data, Nucleic Acids Res. 47 (2019) D847–D852. https://doi.org/10.1093/nar/gky842.
[101] C. Trapnell, A. Roberts, L. Goff, G. Pertea, D. Kim, D.R. Kelley, H. Pimentel, S.L. Salzberg, J.L. Rinn, L. Pachter, Differential gene and transcript expression analysis of RNA-seq experiments with TopHat and cufflinks, Nat. Protoc. 7 (2012) 562–578, https://doi.org/10.1038/nprot.2012.016.
[102] I. Antonov, A. Coakley, J.F. Atkins, P.V. Baranov, M. Borodovsky, Identification of the nature of reading frame transitions observed in prokaryotic genomes., Nucleic Acids Res. 41 (2013) 6514–30. https://doi.org/10.1093/nar/gkt274.
[103] N. Gupta, L.W. DeMong, S. Banda, P.R. Copeland, Reconstitution of selenocysteine incorporation reveals intrinsic regulation by SECIS elements, J. Mol. Biol. 425 (2013) 2415–2422, https://doi.org/10.1016/j.jmb.2013.04.016.
[104] M.T. Howard, B.H. Shirts, L.M. Petros, K.M. Flanigan, R.F. Gesteland, J.F. Atkins, Sequence specificity of aminoglycoside-induced stop condon readthrough: potential implications for treatment of Duchenne muscular dystrophy, Ann. Neurol. 48 (2000) 164–169. http://www.ncbi.nlm.nih.gov/pubmed/10939566. (Accessed 25 July 2019).
[105] S. Ashraf, L. Huang, D.M.J. Lilley, Sequence determinants of the folding properties of box C/D kink-turns in RNA, RNA. 23 (2017) 1927–1935, https://doi.org/10.1261/rna.063453.117.
[106] T.A. Goody, S.E. Melcher, D.G. Norman, D.M.J. Lilley, The kink-turn motif in RNA is dimorphic, and metal ion-dependent, RNA. 10 (2004) 254–264, https://doi.org/10.1261/rna.5176604.
[107] J.E. Fletcher, P.R. Copeland, D.M. Driscoll, A. Krol, The selenocysteine incorporation machinery: interactions between the SECIS RNA and the SECIS-binding protein SBP2, RNA. 7 (2001) 1442–1453. http://www.pubmedcentral.nih.gov/articlerender.fcgi?artid=1370188&tool=pmcentrez&rendertype=abstract. (Accessed 25 September 2013).
[108] K. Caban, S.A. Kinzy, P.R. Copeland, The L7Ae RNA binding motif is a multifunctional domain required for the ribosome-dependent Sec incorporation activity of Sec insertion sequence binding protein 2, Mol. Cell. Biol. 27 (2007) 6350–6360, https://doi.org/10.1128/MCB.00632-07.
[109] L. Fu, B. Niu, Z. Zhu, S. Wu, W. Li, CD-HIT: accelerated for clustering the next-generation sequencing data, Bioinformatics. 28 (2012) 3150–3152, https://doi.org/10.1093/bioinformatics/bts565.